CEN

WORKSHOP

AGREEMENT

CWA 17938

November 2023

ICS 13.100; 13.180

English version

Guideline for introducing and implementing real-time instrumental-based tools for biomechanical risk assessment

This CEN Workshop Agreement has been drafted and approved by a Workshop of representatives of interested parties, the constitution of which is indicated in the foreword of this Workshop Agreement.

The formal process followed by the Workshop in the development of this Workshop Agreement has been endorsed by the National Members of CEN but neither the National Members of CEN nor the CEN-CENELEC Management Centre can be held accountable for the technical content of this CEN Workshop Agreement or possible conflicts with standards or legislation.

This CEN Workshop Agreement can in no way be held as being an official standard developed by CEN and its Members.

This CEN Workshop Agreement is publicly available as a reference document from the CEN Members National Standard Bodies.

CEN members are the national standards bodies of Austria, Belgium, Bulgaria, Croatia, Cyprus, Czech Republic, Denmark, Estonia, Finland, France, Germany, Greece, Hungary, Iceland, Ireland, Italy, Latvia, Lithuania, Luxembourg, Malta, Netherlands, Norway, Poland, Portugal, Republic of North Macedonia, Romania, Serbia, Slovakia, Slovenia, Spain, Sweden, Switzerland, Türkiye and United Kingdom.

EUROPEAN COMMITTEE FOR STANDARDIZATION
COMITÉ EUROPÉEN DE NORMALISATION
EUROPÄISCHES KOMITEE FÜR NORMUNG

CEN-CENELEC Management Centre: Rue de la Science 23, B-1040 Brussels

Ref. No.:CWA 17938:2023 E

Contents

Page

European foreword

This CEN Workshop Agreement (CWA 17938:2023) was developed in accordance with the CEN-CENELEC Guide 29 "CEN/CENELEC Workshop Agreements – A rapid prototyping to standardization" and with the relevant provisions of CEN/CENELEC Internal Regulations — Part 2. It was approved by a Workshop of representatives of interested parties on 2023-09-27, the constitution of which was supported by CEN following the public call for participation made on 2022-09-07. However, this CEN Workshop Agreement does not necessarily include all relevant stakeholders.

The final text of this CEN Workshop Agreement was provided to CEN for publication on 2023-10-10.

Results incorporated in this CWA received funding from the European Union's Horizon 2020 research and innovation program under grant agreement No. 871237 (SOPHIA —Socio-Physical Interaction Skills for Cooperative Human–Robot Systems in Agile Production).

The following organizations and individuals developed and approved this CEN Workshop Agreement:

— Confederation of Danish Industry — DI / Kåre Sørensen

— Human Factors and Ergonomics Society — HFES / Robert Fox

— Institut National de Recherche et de Sécurité — INRS / Chris Hayot

— Italian Institute of Technology — IIT / Arash Ajoudani, Emir Mobedi, Marta Lorenzini

— National institute for insurance against accidents at work — INAIL / Alberto Ranavolo, Giorgia Chini, Alessio Silvetti, Tiwana Varrecchia

— NEN/ CEN/ISO / Aleid Ringelberg

— Società Italiana di Ergonomia — SIE / Francesco Draicchio

— Spanish National Research Council CSIC / David Rodriguez Cianca, Diego Torricelli

— Vrije Universiteit Brussel — VUB / Tom Turcksin

Attention is drawn to the possibility that some elements of this document may be subject to patent rights. CEN-CENELEC policy on patent rights is described in CEN-CENELEC Guide 8 "Guidelines for Implementation of the Common IPR Policy on Patent". CEN shall not be held responsible for identifying any or all such patent rights.

Although the Workshop parties have made every effort to ensure the reliability and accuracy of technical and nontechnical descriptions, the Workshop is not able to guarantee, explicitly or implicitly, the correctness of this document. Anyone who applies this CEN Workshop Agreement shall be aware that neither the Workshop, nor CEN, can be held liable for damages or losses of any kind whatsoever. The use of this CEN Workshop Agreement does not relieve users of their responsibility for their own actions, and they apply this document at their own risk. The CEN Workshop Agreement should not be construed as legal advice authoritatively endorsed by CEN/CENELEC.

Introduction

The European research project SOPHIA aims to develop a new generation of human–robot collaboration (HRC) technologies able to improve human ergonomics during the execution of manual material handling (MMH) activities.

In this regard, several project partners conceived and developed a new instrumental-based tool for monitoring human physical states and identifying biomechanical risk in real-time.

The rationale behind these research activities is the need to strengthen prevention pathways for work-related musculoskeletal disorders (WMDs) and consists of three main reasons [1]:

— to support some of the traditional methods listed within the ISO 11228 — parts 1 to 3, ISO 11226, the technical reports ISO/TR 12295, ISO/TR 12296, and the EN 1005 — Parts 1 to 5 in measuring specific parameters (i.e., loads distances and displacements, forces, frequencies, joint angles, etc.) which in turn define multipliers and/or addends used in equations, to provide risk level scores;

— to directly classify the biomechanical risk by using both intelligent wearable sensors for worker monitoring [2], [3] and alerting [4] and artificial intelligence (AI) algorithms [5], [6];

— to facilitate the classification of the biomechanical risk within the new Industry 4.0 scenario which makes the traditional methods for risk assessment increasingly difficult to apply. Indeed, the presence of new human augmentation technologies [7] such as wearbots (i.e. exoskeletons) and collaborative robots (cobots) in many MMH activities is not currently included in the standards with the consequent difficulty of associating a biomechanical risk with these tasks. If it is, it is only partially so. This also makes it possible to assess the quality of human-robot interaction in terms of benefits and possible emerging risks.

Innovative methods that widen the range of alternatives for biomechanical risk assessment may make it possible to plan and evaluate the effectiveness of specific ergonomic interventions. These tools will enrich the strategies available to the small and medium-enterprises and the large industry and their organizations to improve the daily life activities at work by reducing the WMDs incidence and prevalence, associated costs, sick leave and disability in many occupational populations and determining a positive impact on the health and productivity of employees[1].

The research activities should address the gap, despite the fact that the technologies have a high readiness, that it is still not possible to make quantitative and real-time assessments of the biomechanical risk of all MMH activities including heavy manual lifting, upper extremity repetitive work, computer work and awkward body postures using intelligent sensor networks.

[1] Currently, there are other research groups around the world that are studying instrumental approaches for the assessment of the worker's physical effort in MMH activities. Furthermore, there are a large number of technologies that can be used. For these reasons, this document provides guidelines focusing on what the SOPHIA project and the INAIL group have produced over the years.

1 Scope

This document defines a guideline for establishing and executing an instrumental-based approach for data collection regarding human load during the execution of MMH activities, both with and without HRC technologies support. The guideline describes all necessary requirements and procedures to be used for recording and monitoring data leading to a quantitative risk assessment.

This document focuses on performing an assessment of the biomechanical risk in real-time. This is applicable for simple work activities such as lifting heavy loads, pushing and pulling, overhead work and repetitive movements and exertions of the upper limbs. Any task requiring the application of force by a person to lift, lower, push, pull, hold, or restrain something is referred to as a simple manual handling work activity. This document is not applicable to a real-time risk assessment for multiple work activities because a "post-processing" phase of the acquired signals is needed. Multiple work activities are defined as such when workers rotate between a series of slots, tasks or elements at set time intervals during the course of a work shift or when workers are involved in different types of activities (e.g. lifting, lowering, carrying, pushing, etc). Multiple work activities determine an additive effect of different tasks performed in an eight-hour day.

As these approaches have a considerable technical and computational complexity in their structure, the document defines the materials and procedures to be used to perform a proper and simple real-time or off-line instrumental-based biomechanical risk assessment.

The performed assessment represents only an estimation to show the potential of monitoring human loads by the developed approaches.

This document gives guidance to perform a biomechanical risk assessment by the monitoring of occupational activities directly at the workplace in the real work environment. It does not apply to laboratory work in simulated settings, and it is applicable for direct evaluations and for rating standard methods for biomechanical risk assessment.

The instrumental-based tools use a new generation of wearable sensors and machine learning algorithms to detect the biomechanical risk levels currently indicated by some of the methods listed within the ISO 11228 series, ISO 11226 and the technical report ISO/TR 12295 and the EN 1005 series. The performed assessment represents only an estimation to show the potential of monitoring human loads by the developed approaches. This document does not specify limit values for assessing biomechanical risk which could be included in following standardization activities.

This document can be applied by all individuals who work in the field of occupational health and safety, particularly those involved in the prevention of WMDs through proper biomechanical risk assessment, ergonomic intervention planning, and effectiveness evaluation. The guidelines in the document may be useful to and applied by professionals such as occupational health and safety technicians, ergonomists, and occupational physicians. In addition, it could be used by members of technical committees involved in writing and/or modifying ergonomic standards.

This document does not define ethical and worker acceptance considerations.

2 Normative references

The following documents are referred to in the text in such a way that some or all of their content constitutes requirements of this document. For dated references, only the edition cited applies. For undated references, the latest edition of the referenced document (including any amendments) applies.

EN 1005-1:2001, *Safety of machinery —Human physical performance —Part 1: Terms and definitions*[2]

[2] As impacted by EN 1005-1:2001/A1:2008.

EN 1005-2:2003, *Safety of machinery —Human physical performance —Part 2: Manual handling of machinery and component parts of machinery*[3]

EN 1005-3:2002, *Safety of machinery — Human physical performance — Part 3: Recommended force limits for machinery operation*[4]

EN 1005-4:2005, *Safety of machinery — Human physical performance — Part 4: Evaluation of working postures and movements in relation to machinery*[5]

EN 1005-5:2007, *Safety of machinery — Human physical performance — Part 5: Risk assessment for repetitive handling at high frequency*

ISO 11228-1:2021, *Ergonomics — Manual Handling — Part 1: Lifting, Lowering and Carrying*

ISO 11228-2:2007, *Ergonomics — Manual Handling — Part 2: Pushing and Pulling*

ISO 11228-3:2007, Ergonomics — Manual Handling — Part 3: Handling of low loads at high frequency[6]

ISO/TR 12295:2014, *Ergonomics — Application Document for ISO Standards on Manual Handling (ISO 11228-1, ISO 11228-2 and ISO 11228-3) and Static Working Postures (ISO 11226)*

ISO/TR 12296:2012, *Ergonomics — Manual handling of people in the healthcare sector*

ISO 11226:2000, *Ergonomics — Evaluation of Static Working Postures*[7]

ISO 10218-2:2011, *Robots and robotic devices — Safety requirements for industrial robots — Part 2: Robot systems and integration*

3 Terms and definitions

For the purposes of this document, the following terms and definitions apply.

ISO and IEC maintain terminology databases for use in standardization at the following addresses:

— ISO Online browsing platform: available at https://www.iso.org/obp/

— IEC Electropedia: available at https://www.electropedia.org/

3.1
human–robot collaboration
HRC
interaction that refers to a cooperative interaction between humans and robots in shared workspaces or environments

Note 1 to entry: The main objective is to integrate human capabilities, such as perception, decision-making, and dexterity, with the strengths of robots, such as precision, strength, and endurance, to create a symbiotic relationship between humans and robots, where they work together to enhance overall productivity, efficiency, and safety.

[3] As impacted by EN 1005-2:2003/A1:2008.
[4] As impacted by EN 1005-3:2002/A1:2008.
[5] As impacted by EN 1005-4:2005/A1:2008.
[6] A revision of the document with the new title „*Ergonomics — Manual handling — Part 3: Handling of low loads at high frequency*“ is planned
[7] As impacted by ISO 11226:2000/Cor 1:2006.

Note 2 to entry: In scientific literature, HRC is presented in various forms, such as Coexistence, Cooperation, and Communication, however, they all share the main aspects and objectives described above.

3.2
Work-related Musculoskeletal Disorders
WMDs
group of inflammatory and degenerative diseases associated to MMH activities that affect the peripheral nerves, ligaments, tendons, muscles, cartilage, spinal discs and upper and lower limb joints

Note 1 to entry: Unfavourable work conditions, can worsen or prolong WMDs symptoms, which are significantly influenced by the work environment and performance.

[SOURCE: [8]]

3.3
Manual Material Handling activity
MMH activity
any occupational activity requiring the use of human force to lift, lower, carry or otherwise move or restrain an object.

Note 1 to entry: Analysed within the ergonomic standards of the ISO 11228 series, ISO 11226, the technical reports ISO/TR 12295 and ISO/TR 12296 and the EN 1005 series.

Note 2 to entry: It includes lifting and carrying heavy loads, pushing and pulling, upper extremity repetitive motion or work and overhead work activities.

[SOURCE: EN 1005-1:2001, definition 3.8, modified – occupational and notes has been added, [9]]

3.4
artificial intelligence
AI
engineered system that generates outputs such as content, forecasts, recommendations or decisions for a given set of human-defined objectives

Note 1 to entry: The engineered system can use various techniques and approaches related to artificial intelligence to develop a model to represent data, knowledge, processes, etc. which can be used to conduct tasks.

Note 2 to entry: AI systems are designed to operate with varying levels of automation.

[SOURCE: ISO/IEC 22989:2022, definition 3.1.4]

3.5
neural network
NN
neural net
artificial neural network
<artificial intelligence> network of one or more layers of neurons connected by weighted links with adjustable weights, which takes input data and produces an output

Note 1 to entry: Neural networks are a prominent example of the connectionist approach.

Note 2 to entry: Although the design of neural networks was initially inspired by the functioning of biological neurons, most works on neural networks do not follows that inspiration anymore.

[SOURCE: ISO/IEC 22989:2022, definition 3.4.8]

3.6
machine learning algorithm
program able to “learn” from input available to them

Note 1 to entry: The input to a learning algorithm is training data, representing experience, and the output is some expertise, which usually takes the form of another computer program that can perform some task.

[SOURCE: [10]]

3.6.1
learning
acquiring knowledge, behaviour, skills, values, preferences or understanding

[SOURCE: ISO 29995:2021, 3.3.2]

3.7
wearable sensor
devices able to produce an output signal for the purpose of sensing the behaviour of bone segments and joints, the forces that humans exchange with the environment and the activities of muscles

Note 1 to entry: The term wearable indicates that these sensors need to be placed on the human body (worn). When the sensors are wearable the term “wearable” means “miniaturized (light weight and small-size)”, “wireless connected”.

3.8
real-time instrumental-based tool for biomechanical risk assessment
procedure that uses sensors, algorithms and indicators for human movement/effort monitoring and biomechanical risk level estimation in real-time (online, streaming)

Note 1 to entry: The notation 'online' is used with the same meaning as in computer science, i.e. as the estimation of the level of biomechanical risk in direct and constant connection to wearable sensors for movement measuring.

Note 2 to entry: The tool is intended to provide a biomechanical risk assessment directly in the workplace and not in the laboratory in simulated settings.

Note 3 to entry: Streaming is a direct and constant connection, via a telematics network, between the wearable sensors (sources) and the software interface of the biomechanical classifier (destination).

[SOURCE: [2],[3]]

3.9
kinematics
study of the motion of trunk, head and lower and upper limb segments and joints in three-dimensional space, using only the notions of space and time, regardless of the causes (forces) that generate the motion itself

[SOURCE: [11], [12], [13]]

3.10
kinetics
study of the effects of forces on the movement of material bodies’

[SOURCE: [14]]

3.11
surface electromyography
non-invasive instrument that allows to study the behaviour of the activations of muscles

[SOURCE: [15], [16], [17], [18], [19], [20], [21], [22]]

3.12
inertial measurement unit
IMU
electronic device composed of accelerometers, gyroscopes and magnetometers that measure-acceleration, orientation and angular rates of change

Note 1 to entry: Inertial describes the resistance to motion (inertia) of a free mass that has been accelerated by an external force or torque since these sensors work on the inertia principle.

3.13
3D depth camera
imaging instrument that allows images to approximate three dimensions as perceived by human binocular vision in terms of depth perception

Note 1 to entry: A single lens that changes position is used by some 3D cameras, while others employ two or more lenses to record different points of view.

3.14
sensorized shoe and insole
wearable wireless measurement sensor/tool for real-time sensing foot dynamics (pressures and forces)

Note 1 to entry: Many of them come equipped with IMU.

3.15
bipolar sEMG Sensor
sensor that measures the electrical activity of the muscles involved in a specific movement using wet electrodes placed on the skin

[SOURCE: [15-22]]

3.16
Multi-channel sEMG
High-density sEMG
HDsEMG
instrumental method that uses linear and two-dimensional electrode arrays, to analyze the instantaneous potential maps, decompose the sEMG signals to obtain the motor unit action potential's firing rate and estimate the myoelectric manifestation of muscle fatigue.

[SOURCE: [15-22]]

3.17
dynamometer
strain gauge
basic instrument used to measure the muscle strength of a subject's body part

3.18
Center of Pressure
CoP
point of application of the ground reaction force

4 Characteristics of Online instrumental-based tools for biomechanical risk assessment

Human movement monitoring technologies offer the possibility of an in-depth assessment of the worker's physical effort during the execution of MMH activities defined in ISO 11228-1:2021, ISO 11228-2:2007, ISO 11228-3:2007, ISO/TR 12295:2014 and ISO 11226:2000. For this reason, they allow a static and dynamic postural assessment (kinematic analysis), of the forces that the worker exchanges with the work environment (kinetic analysis) and of muscular behaviour (surface electromyographic analysis).

The technologies used shall comply with ISO 10218-2:2011 and EN 1005-1:2001+A1:2008, EN 1005-2:2003+A1:2008, EN 1005-3:2002+A1:2008, EN 1005-4:2005+A1:2008, EN 1005-5:2007 and should allow the natural motor strategy by the worker allowing a monitoring of occupational activities in the real work environment.

These approaches can operate for both direct evaluations and for rating standard methods for biomechanical risk assessment by measuring all the parameters needed to assess the risk.

Direct instrumental evaluations can be used

— for sensor-based biomechanical risk assessments when existing methods are not usable or,

— when usable, to obtain confirmation of their validity.

Validated algorithms and indicators can be used. The rating of standard methods can be used to measure some parameters, otherwise measured with lower precision and accuracy, necessary to obtain the level of risk.

NOTE The hardware and software systems that make up the instrumental tool are always referred to a good mobile system and a gold standard movement analysis system to validate the required accuracy with standardized accuracy in time and measured metric.

Biomechanical risk assessment using sensors will have to be extremely simple and all efforts in the coming months/years will have to go in this direction. The use of 3D depth cameras for kinematic data acquisition may be a very good solution. It will be useful and important to develop systems for real-time assessment of complex work in addition to simple work.

In this document, there are no considerations on ethical aspects and acceptance by workers.[8]

5 Hardware description

5.1 General

A sensors network shall be used for a full biomechanical risk assessment at workplace.

Only technologies capable of making data available instantaneously shall be considered for movement monitoring, HRC technologies controlling and workers alerting.

[8] The European research project SOPHIA is addressing this issue in detail and important results will be published in the near future.

This consists of the following devices (Figure 1):

— Wireless wearable IMUs (Figure 1 a)),

— 3D depth cameras (Figure 1 b)),

— Force measuring devices/force gauges (Figure 1 c)),

— sensorized insoles and shoes (Figure 1 d)),

— bipolar sEMG (Figure 1 e)),

— HDsEMG (Figure 1 f)).

Figure 1 — IMUs a), 3D depth cameras b), Force measuring devices c), sensorized insoles d), bipolar e) and HDsEMG f)

These devices enable a detailed estimation of kinematics, kinetics, and muscle behaviours.

All devices shall

— be compatible with Personal Protective Equipments (PPEs)/Individual Protection Equipments (IPEs),

— have a minimum interference with workers' normal movements at their workplaces [2], [3].

These wearable sensors are placed on the workers' body. Based on the MMH activity to be evaluated, different sensor setups shall be selected.

All devices alone or in combination can measure and estimate, among the other, the following parameters:

— joint angles in the sagittal, frontal and horizontal planes;

— linear and angular velocities;

— linear and angular accelerations;

— forces, joint torques and powers;

— muscle activities, co-activations, muscle fatigue.

All sensors shall be synchronized for data alignment in time. Wireless protocols such as Wi-Fi and Bluetooth should be used to establish a connection.

NOTE Wi-fi sends data faster and further than Bluetooth but consumes more power.

The devices used for workers monitoring should be reliable. In particular, sensors for the study of kinematics such as IMUs and 3D depth cameras should have been validated through a comparison with gold standard reference systems such as optoelectronics. [23], [24], [25], [26]

5.2 Purpose of Sensors for kinematics

IMUs

IMUs make it possible to measure and estimate the position, orientation, velocity and acceleration, of each segment under study[9].

Three orthogonal accelerometers and three orthogonal gyroscopes are used to detect the linear acceleration and angular velocity along three orthogonal axes. Angles and positions are obtained via numerical integration.

Tri-axial magnetic sensors can be added to IMUs as well, although their use in the workplace is more critical because of the possible existence of electromagnetic fields.

3D depth cameras

3D depth cameras can be used for imaging instruments that allow images to approximate three dimensions as perceived by human binocular vision in terms of depth perception. A single lens that changes position is used by some 3D cameras, while others employ two or more lenses to record different points of view. 3D depth cameras are used for joint angles measurements.

Force measuring devices/force gauges

A force gauge shall be used to measure the muscle strength of a subject's body part while it is held in place. Force gauges with high levels of sensitivity and inter-examiner reliability can be used to detect both force and angle.

Superior grip dynamometers can also be used to measure forces. Their application is limited to specific hand sizes and cannot be used to measure forces from many fingers at once.

Multi-dimensional instrumented gloves can also be used for the measurement of grip forces and fatigue.

Sensorized shoes and insoles

Sensorized shoes and insoles can be used to measure pressures and forces on the foot dynamics. They can be used in combination with IMU.

5.3 Purpose of Sensors for sEMG

Bipolar sEMG Sensors

Bipolar sEMG can be applied for the measurement of the electrical activity of the muscles involved in a specific movement using wet electrodes placed on the skin. Among the parameters and indexes used to estimate muscle behaviours, the “activation timing”, the “amplitude (maximum values, average rectified values or ARVs, root mean square or RMS)”, “co-activations” and “muscle fatigue” are the most useful in ergonomics.

[9] The literature uses a range of uniaxial to triaxial magnetic sensors, gyroscopes, and accelerometers.

Multi-channels/HDsEMG

Multi-channel/High-density sEMG (HDsEMG) can be performed by using linear or two-dimensional electrode arrays. HDsEMG allows the analysis of the instantaneous potential maps, to decompose the sEMG signals to obtain the motor unit action potentials firing rate, and estimate the myoelectric manifestation of muscle fatigue.

6 Sensors setup and sensors placement

The behaviour of body joints, forces and muscles during work activities depend on the MMH activity. A specific sensor setup shall be selected on the basis of the MMH to be evaluated.

The sensor setup for data acquisition should be chosen with the aim of being comfortable to the worker and must not impede the worker's normal motor strategy that he/she performs during his/her MMH activities.

The number of sensors should be the minimum sufficient for the biomechanical risk assessment.

Kinematics: IMUs

The positioning of IMU sensors can vary significantly as it depends on the MMH activity and body area to be assessed. IMUs can be positioned on the upper limbs, head, trunk and lower limbs.

Depending on the IMU positioning, simplified kinematic protocols should be used for this purpose.

On the other hand, however, using a complete kinematic approach makes it possible to measure the segmental and articular behaviours of the whole body, also allowing the extraction of useful information for the measurement of parameters that are used to quote multipliers and addends within the equations of traditional methods listed within the Ergonomic standards[10]. The segmental and articular behaviours of the whole body can be measured with the complete kinematic approach.

NOTE 1 There are several sensor networks on the market and under development that enable the acquisition of whole-body kinematics.

To minimize skin motion artifact, each mounting system provides a good attachment to the body.

There are different placements for whole body sensor placement.

Two examples for whole body acquisition are described below. For the placement of sensors on the body districts of interest, the use of elastic bands or elastic textile suit should be preferred to other solutions.

EXAMPLE 1 17 IMUs sensors placed either in an elastic textile body suit or in a set of mounting straps as shown by the examples in Figure 2.

The whole-body network setup (Example 1) involves the placement of 17 IMUs:

— feet: bilaterally on the middle of bridge of foot,

— lower legs: bilaterally flat on the shin bone (medial surface of the tibia),

— upper legs: bilaterally on the lateral side above knee,

— pelvis: flat on sacrum,

— sternum: flat, in the middle of the chest,

[10] EN 1005-1:2001+A1:2008, EN 1005-2:2003+A1:2008, EN 1005-3:2002+A1:2008, EN 1005-4:2005+A1:2008, EN 1005-5:2007, ISO 11228-1:2021, ISO 11228-2:2007, ISO 11228-3:2007, ISO/TR 12295:2014 and ISO 11226:2000

— shoulders: bilaterally on the scapula (shoulder blades),

— upper arms: bilaterally on the lateral side above elbow,

— fore arms: bilaterally on the lateral and flat side of the wrist,

— hands: bilaterally backside of hand,

— head: any comfortable position.

NOTE The figure was provided by Movella Technologies BV and shows Xsens MVN Awinda (or MVN Link) by Movella Technologies BV, Enschede. This information is given for the convenience of users of this document and does not constitute an endorsement by CEN of the product named.

Figure 2 — Types of placement of whole body sensors network placement

EXAMPLE 2 11 IMUs sensors placed in a set of mounting straps in sensors network used in SOPHIA project (Figure 3).

The whole-body sensors network setup (Example 2) involves the placement of 11 IMUs:

Bilaterally on:

— lower legs: bilaterally flat on the shin bone (medial surface of the tibia),

— upper legs: bilaterally on the lateral side above knee,

— upper arms: bilaterally on the lateral side above elbow,

— fore arms: bilaterally on the lateral and flat side of the wrist,

— trunk: on the stern and pelvis level,

— head: on the forehead.

Figure 3 — Whole body sensors network used within the SOPHIA project

When using sensor setups for whole-body motion monitoring, it is possible to replicate via software the execution of the work activity with an avatar. Two examples of these are shown in the Figure 4 and 5.

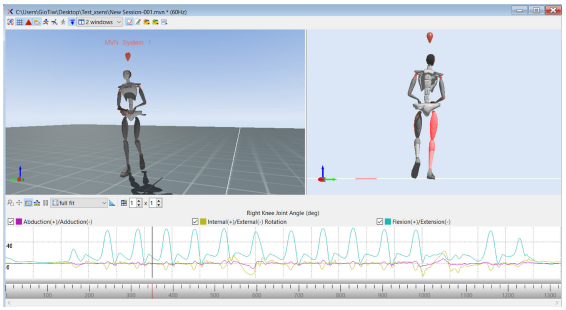

NOTE The figure was provided by Movella Technologies BV and shows Xsens MVN Awinda (or MVN Link) by Movella Technologies BV, Enschede. This information is given for the convenience of users of this document and does not constitute an endorsement by CEN of the product named.

Figure 4 — Avatar and joint angles signals obtained using the sensors network of the EXAMPLE 1

Figure 5 — Avatar of the worker obtained using the sensors network of the EXAMPLE 2

NOTE 2 Optoelectronic systems are the gold standard for measuring kinematics in the laboratory. For these systems, the positioning of retro-reflective markers on anatomical landmarks would need to be further investigated. Such a description is not made in these guidelines due to the choice of describing only technologies that can be easily used in the workplace and are therefore mainly wearable.

sEMG

The sensors should be positioned according to the district of interest. To ensure that the signal quality is not affected by noise, the positioning should follow the indications given in the European Recommendations for Surface Electromyography (SENIAM) [20] and in the Atlas of Muscle Innervation Zones [21] and [27]. [11]

EXAMPLE 3 analysis of a symmetrical heavy lifting activity. Placement of 2 sensors monolaterally on the rectus abdominis superior and erector spinae.

EXAMPLE 4 analysis of an asymmetrical heavy lifting activity. Placement of 4 sensors bilaterally on the rectus abdominis superior and erector spinae.

EXAMPLE 5 analysis of repetitive movements and exertions of the upper limbs or overhead work task. The behaviour of the shoulder, elbow, and wrist muscles should be estimated. Depending on the type of the task, either unilateral or bilateral positioning shall be chosen. The muscles mainly investigated are the trapezius, the three deltoid bundles, the pectoralis, the biceps, and triceps brachii and the flexors and extensors of the fingers.

7 Software interface recommendations for biomechanical risk classification

The software should take into consideration the indices that best reflect the biomechanical risk when performing specific MMH activities

NOTE 1 This was accomplished by considering both earlier research that had been published in international journals before the SOPHIA project [28], [29], [30], [31] as well as new experiments and studies (such as team [32] and fatiguing [33], [34] lifting that we are currently pursuing as part of the SOPHIA project). More information can be found in Annex B.

The biomechanical risk assessment should be performed for all the MMH activities:

— lifting (one- and two-person),

— holding and carrying of objects/items/loads/weights/masses,

— pushing and pulling,

— repetitive movements and exertions of the upper limbs and

— overhead work (Figure 6).

Figure 6 shows a software interface developed in a Matlab environment within the SOPHIA project for the online instrumental-based tool for monitoring and classifying the biomechanical risk with which it is possible to select the task to be analyzed.

[11] The Standards for Reporting sEMG Data, written by Dr. Roberto Merletti, are endorsed by the International Society of Electrophysiology and Kinesiology (ISEK). The standards are also published in the Journal of Electromyography and Kinesiology (JEK) (https://isek.org/emg-standards/).

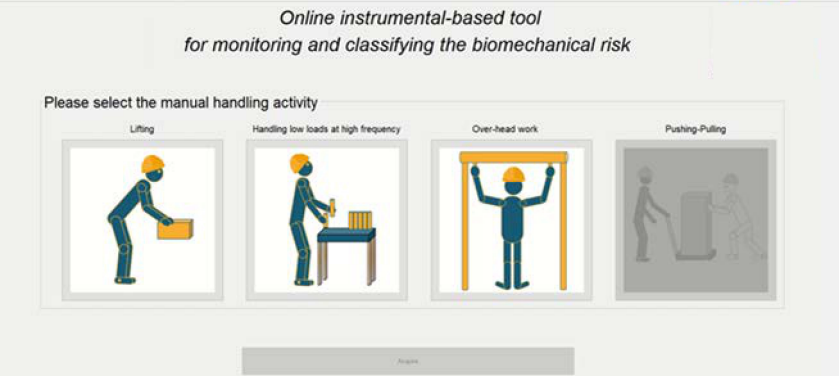

Figure 6 — Software interface for selecting the task to be analyzed

The software should give the options to:

1) Allow the user to select the MMH activity of interest,

2) Enter the worker's information in a database,

3) Create a model of the muscles to investigate or select an existing one among those created (Figure 7 a)) and Figure 8,

NOTE 2 Some software use databases for sensors setup and it gives users the option of choosing pre-existing protocols of the muscles and body segments to be acquired or to create new, fully custom ones.

4) Guide users to apply the sensors correctly according to the selected sensors setup (Figure 7 b)),

5) Select an existing participant or create a new participant with anthropometric data: the system should automatically assigns a progressive identification to the subject to anonymize it (Figure 7 c)),

6) Record the Maximum Voluntary Contraction (MVC) and the experiment signals (Figure 7 c)),

NOTE 3 The MVC is measured and calculated to obtain a reference value for the amplitude normalisation of the sEMG signal acquired during the MMH activity. It is important that this value is correctly and properly quantified, as an error in its estimation could directly propagate to the level of risk. For this reason, it is necessary to measure MVC according to the guidelines on sEMG.

NOTE 4 MVC is needed for the estimation of sEMG and force production of some shoulder muscles [22].

7) Save the data,

8) Show the risk level directly if the assessment is performed in real-time (online) or allow signal processing if the assessment is performed offline. A specific function should be implemented to automatically import all the chosen algorithms and apply them to the collected data,

9) Add new indices to incorporate it into the tool's design.

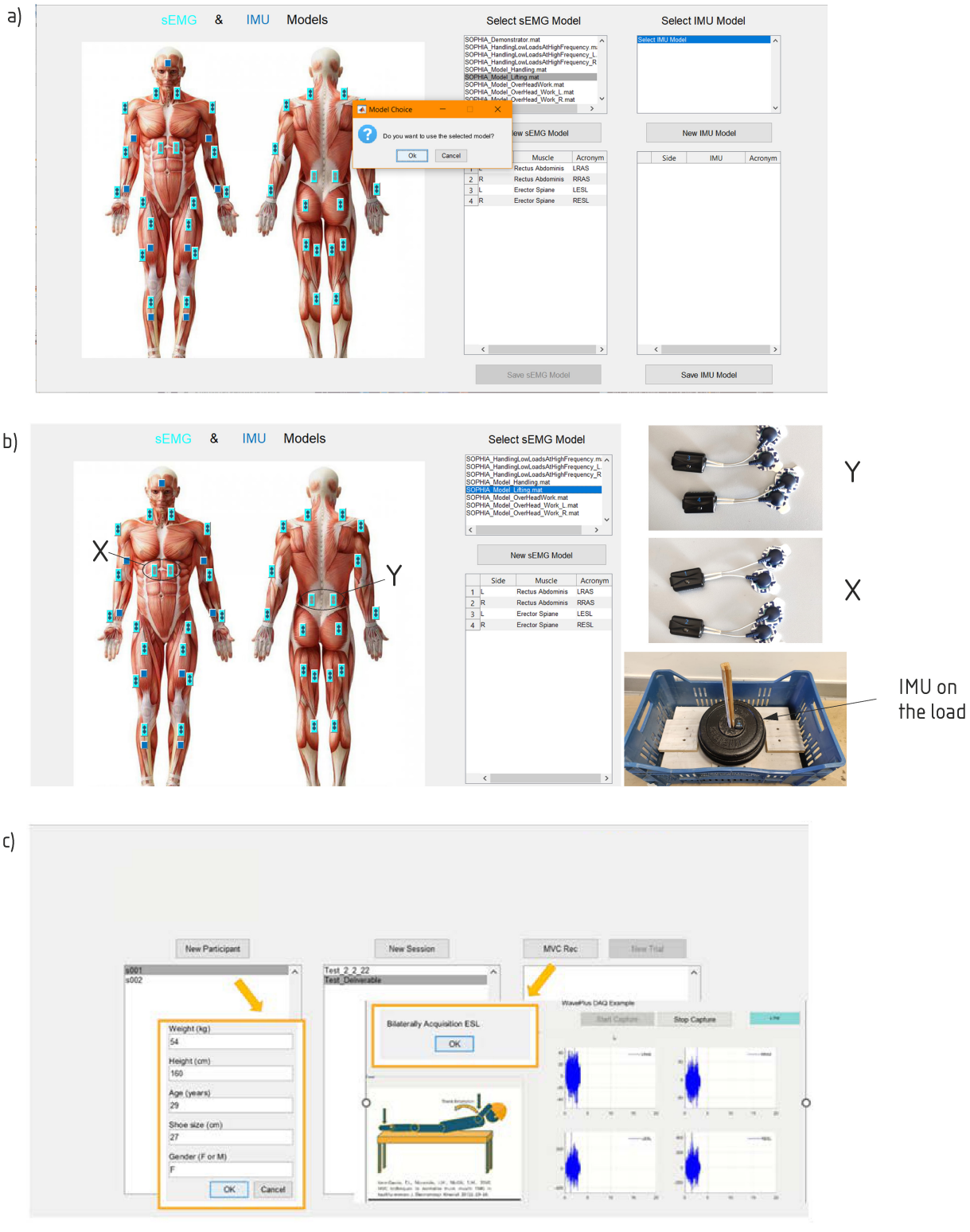

Figure 7 — a) Software interface developed within the SOPHIA project for the creation or selection of a sensor setup. b) Probes applied on the subject's body segments according to the selected sensors setup. c) Entering worker data and selecting the acquisition trial

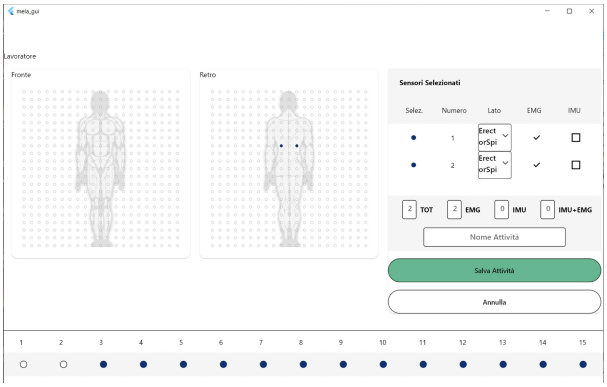

Figure 8 — Software interface developed within the MELA project for the creation or selection of a sensors setup

Application: lifting loads of over 3 kg

The software should be able to segment the task sub-phase (e.g. lifting and lowering) in real-time. The vertical displacement and velocity of the IMU placed above the load shall be determined. To estimate vertical velocity and displacement, the filtered acceleration of IMU load shall be integrated one and two times respectively. The drift should be corrected assuming that before and after lifting the vertical acceleration and speed are zero.

NOTE 5 Filtered by applying a 3rd order low-pass Butterworth filtered with a 10 Hz cut-off frequency.

The lifting and lowering segmentation should be performed by detecting:

— the initiation of the lifting which shall be defined as the time point at which the IMU load velocity exceeded a velocity threshold of 0,025 m/s [30] along the vertical axis;

— the termination of the lifting which shall be defined as the maximum point on the graph of the vertical displacement of IMU load (z axis);

— the termination of the lowering which shall be defined as the point on the graph at which the IMU load velocity fell below the velocity threshold in the opposite direction after the minimum value (Figure 9).

This algorithm shall be applied on small windows (i.e. 200 ms) to find the described events.

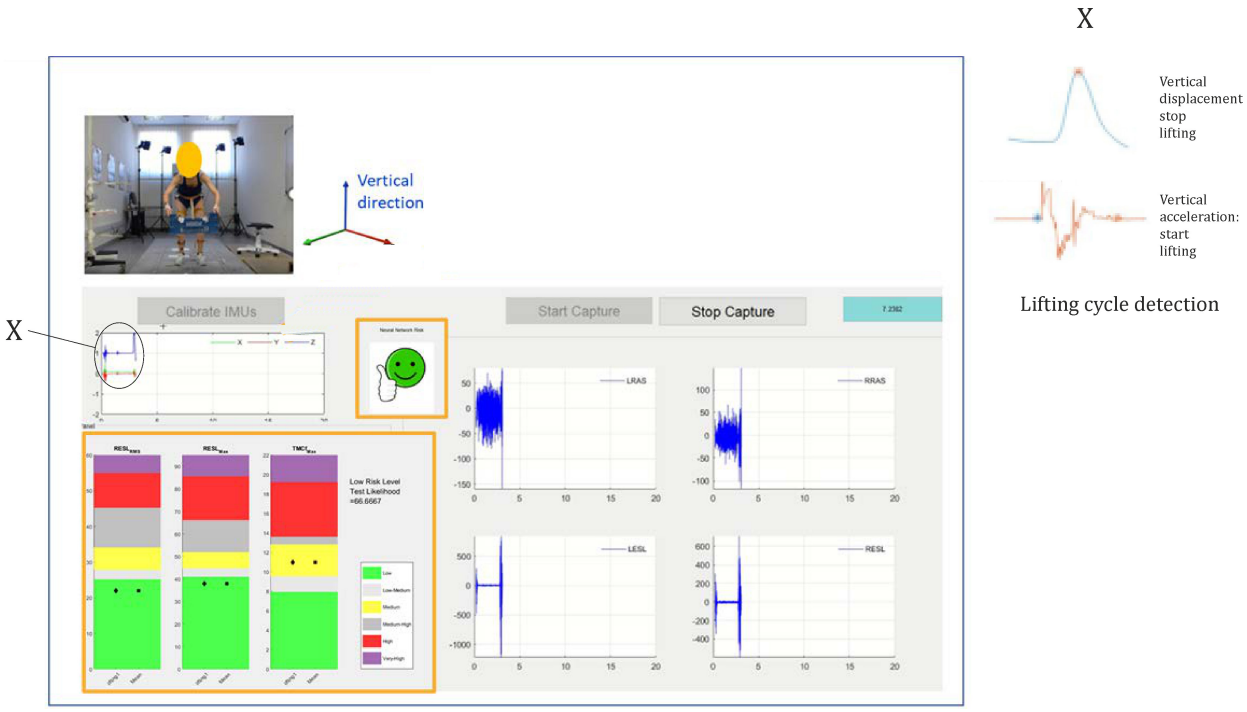

Figure 9 — Software interface developed within the SOPHIA project for lifting and lowering detection and biomechanical risk classification

Direct evaluation: the co-activation of the erector spinae and rectus abdominis muscles enables the classification of biomechanical risk in both single and team lifting and the differentiation of various risk conditions [32, Figure 10 a)]. The forces at the L5-S1 joint correlate with the activation and co-activation of the trunk muscles [28, 32, Figure 10 a)]. In order to correctly acquire abdominal muscles, one should avoid recruiting workers with a high Body Mass Index (BMI) and eliminate any interference from the heart muscle.

NOTE 6 The forces at the L5-S1 joint are the primary cause of Low Back Disorders (LBDs) in lifting activities.

Muscle co-activation [33-34] (Figure 10 c)) and HDsEMG (Figure 10 b)) can be used to significantly discriminate across the different biomechanical risk levels also during fatiguing lifting activities earlier than bipolar sEMG [34].

NOTE 7 Muscle co-activation [33] is higher in people with low back pain (LBP) who adopt a different motor strategy [22]

In fatiguing lifting tasks, kinematic and kinetic indices allow for the differentiation of risk levels and individuals with and without LBP (Figure 10 d)).

EXAMPLE 1 Center of Pressure (CoP) parameters [35]

EXAMPLE 2 Root Mean Square (RMS) activation of the trunk muscles [34]

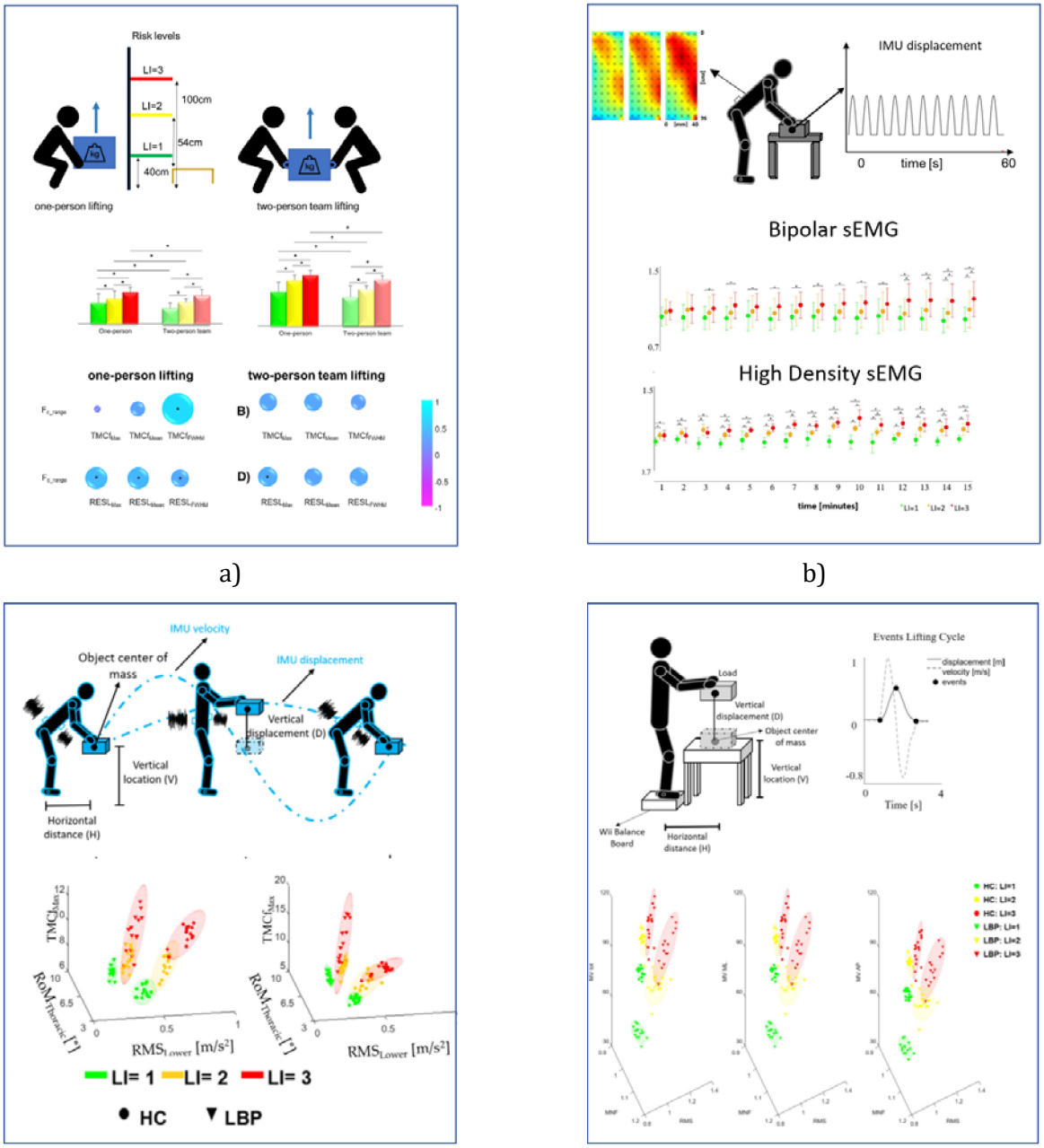

a) b)

c) d)

Figure 10 — Scientific results on a) single and team lifting [32]; b) on fatiguing lifting investigated by using HDsEMG [33]; c) fatiguing lifting investigated by using bipolar sEMG [34] and d) fatiguing lifting investigated by using the CoP [35].

The selected parameters should be evaluated in real-time and the risk level should be estimated using thresholds and ANNs (Figure 9).

Application: repetitive movements and exertions of the upper limbs

For repetitive movements and exertions of the upper limbs the risk level could be computed by a direct instrumental evaluation by using, for instance, the Potvin's method [36], [37] (Figure 11) and by the rating of standard methods using i.e. the IMU sensors setup (to verify, among the others, the RULA/REBA score and OCRA approach).

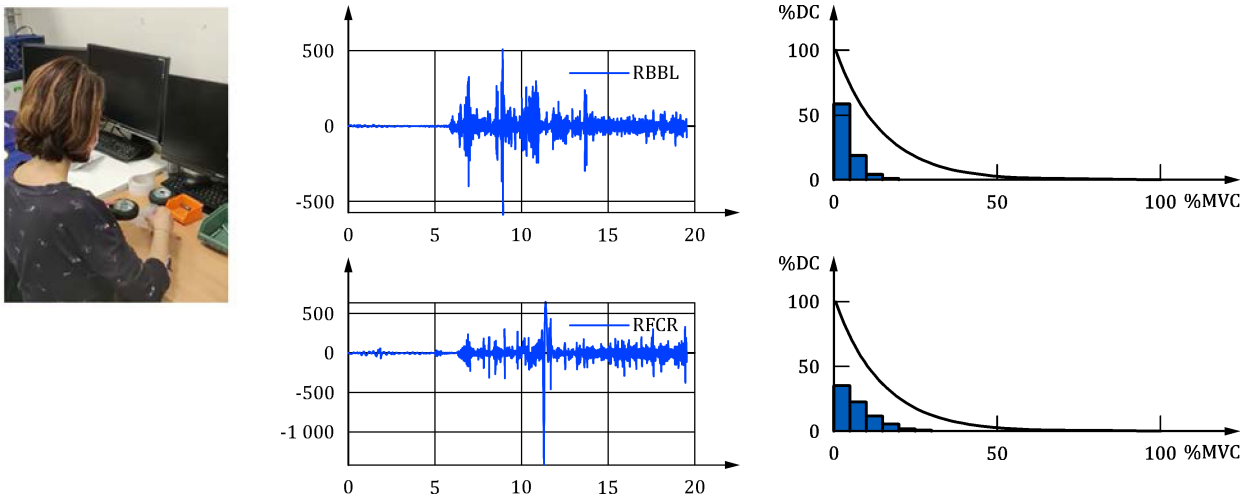

Figure 11 — Acquisition, raw signals a) and risk classification b) for repetitive movements and exertions of the upper limbs c)

Application: Overhead work

The overhead work shall be evaluated by the Potvin's method [36], [37] and the Joint Analysis of EMG Spectrum and Amplitude (JASA) method [38] (Figure 12).

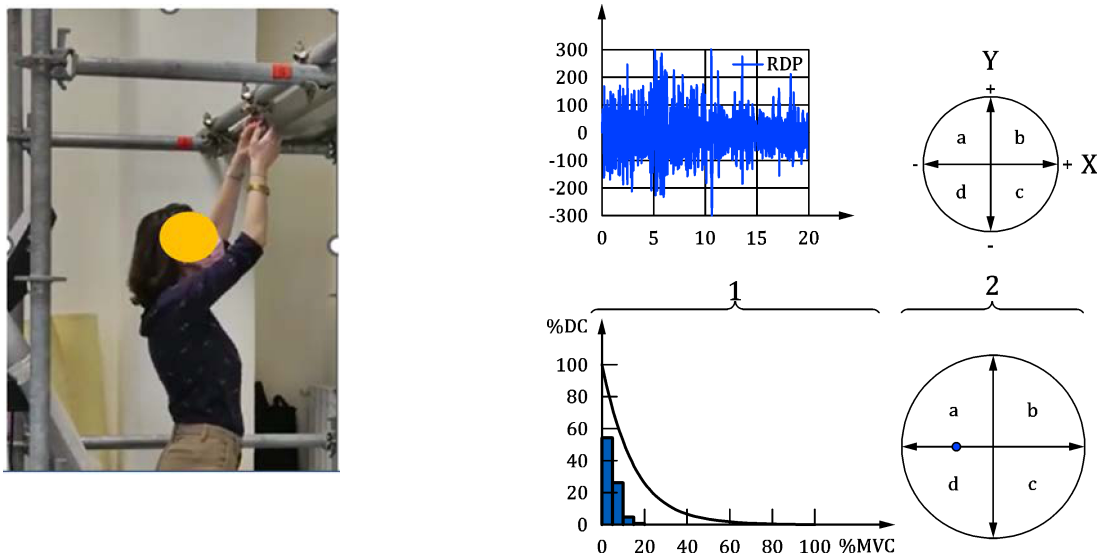

Key

1	Potvin RDP	a	recovery
2	Jasa RDP	b	force increase
X	temporal change in EA	c	fatigue
Y	temporal change in MF	d	force decrease

Figure 12 — Acquisition, raw signals and risk classification a) for overhead work b)

8 Data processing and indices

8.1 Kinematic data

IMUs can be used for monitoring joint behaviours and the body Center of Mass (CoM). Along with acquiring accelerations from each IMU sensor during the tasks, the following stability parameters can be evaluated:

— the root mean square (RMS) of each component of the acceleration (RMSacc_x, RMSacc_y, RMSacc_z),

— the RMS of the acceleration magnitude (RMSacc_magnitude) and

— the RMS of the jerk (i.e. the derivative of the acceleration) magnitude (RMSjerk) [39], [40].

Using the kinematic data, the joint angles and the angular jerk (can be calculated in real-time by the third derivative over time of the angle displacement [degrees/s3]. The jerk square mean (JSM) value is an index of smoothness of the movement.

NOTE 1 The lower the Jerk the smoother the movements [40].

The JSM values can be evaluated for each joint as follows:

$$\mathrm{JSM} = \frac{1}{\mathrm{n}}\sum_{\mathrm{i}=1}^{\mathrm{n}} J_i^2$$

where

JSM is the jerk square;

J_i is the instantaneous value of the jerk;

n is the total number of data points.

NOTE 2 In lifting tasks the JSM correlates with risk levels in lifting tasks [5].

From kinematic data, the CoM values can be computed as the centroid of a set of elements composed by p body segments. The computation can be carried on by considering kinematic and anthropometric data together with the body segment parameters, according to the weighted average of the individual body segments' center of mass [41], [42]:

$$CoM_x = \frac{1}{m}\sum_{i=1}^{p} x_i * m_i$$

$$CoM_y = \frac{1}{m}\sum_{i=1}^{p} y_i * m_i$$

$$CoM_z = \frac{1}{m}\sum_{i=1}^{p} z_i * m_i$$

where

CoM_X is the instantaneous x components of the CoM position;

CoM_y is the instantaneous y component of the CoM position;

CoM_Z is the instantaneous z component of the CoM position;

m is the mass of the system considered (i.e. upper or whole body);

p is the number of segments considered;

x_i, y_i, z_i are the components of the CoM position of the i-th segment;

m_i is the mass of the i-th segment.

Then, for each of the CoMs calculated, the kinetic energy (E_k) during the tasks can be calculated as the sum of the kinetic energy on the x (E_{kx}), y (E_{ky}) and z (E_{kz}) axes as follows:

$$E_k = E_{kx} + E_{ky} + E_{kz} = \frac{1}{2} m \left(v_x^2 + v_y^2 + v_z^2 \right)$$

where

E_k is kinetic energy;

m is mass of the CoM considered;

v_x is the velocity component on x of the CoM considered;

v_y is the velocity component on y of the CoM considered;

v_z is the velocity component on z of the CoM considered.

NOTE 3 The centrifugal kinetic energy components have been ignored.

The potential energy (E_p) can be calculated using the following equation:

$$E_p = mgh$$

where

E_p is potential energy;

h is the vertical (y) component of the CoM of the system considered;

g is the acceleration of gravity.

The mechanical energy (E_M) can be calculated as follows:

$$E_M = E_k + E_p$$

For each CoM, the difference between maximum and minimum values of each E_k, E_p and E_M within the task can be considered as Lifting Energy Consumption (LEC) (LECk, LECp and LECM, respectively) [30]. During lifting tasks, these indexes, referring respectively to the load (CoML), the multi-segment upper body model (head, trunk, upper arms, forearms, and hands) and load together (CoMUpp+L). The whole body (multi-segment upper body model, pelvis, thighs, shanks, and feet) and load (CoMTot) are related to the risk levels [30] (Figure 13).

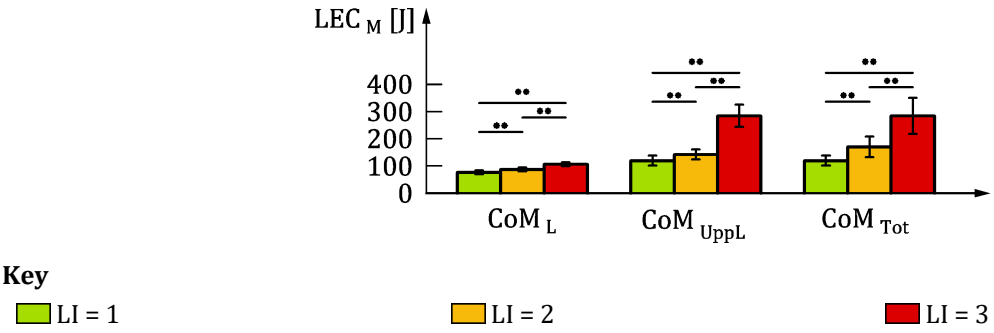

Figure 13 — Means and standard deviations of the LEC_M

The means and standard deviations of the LECM are calculated while performing manual material lifting tasks in the three different conditions (LI = 1, LI = 2 and LI = 3).

The different conditions include the three CoMs of the load (CoML): the multi-segment upper body model (CoMUpp considering head, trunk, upper arms, forearms and hands), the whole body (multi-segment upper body model, pelvis, thighs, shanks and feet) and load (CoMTot).

NOTE 4 ** Significant differences at the post hoc analysis with $p < 0.001$ [30].

NOTE 5 In order to identify occupational lifting activities with a high risk of low back diseases it is possible to use, among other approaches, the Revised NIOSH Lifting Equation (RNLE).

Kinematic data can be used by the software for rating Revised NIOSH Lifting Equation (RNLE) multipliers from the measurement, with IMU sensors, of the parameters required.

EXAMPLE See Annex A for mathematical description.

8.2 Kinetic data: Forces and moment at the L5-S1 joint

The net reaction forces (F_{L5-S1}) and moments (M_{L5-S1}) at the L5-S1 joint can be calculated in the Global laboratory Reference System according to the dynamic multi-segment using the following formulas [43]:

$$\overrightarrow{F_{L5-S1}} = -\sum_{j=1}^{n} \overrightarrow{F_j} + \sum_{i=1}^{p} m_i \vec{g} + \sum_{i=1}^{p} m_i \overrightarrow{a_i}$$

$$\overrightarrow{M_{L5-S1}} = -\sum_{j=1}^{n} \left(\overrightarrow{r_j} - \overrightarrow{r_{L5-S1}} \right) \times \overrightarrow{F_j}$$

$$+\sum_{i=1}^{p} \left(\overrightarrow{r_i - r_{L5-S1}} \right) \times m_i \vec{g} + \sum_{i=1}^{p} \left(\overrightarrow{r_i - r_{L5-S1}} \right) \times m_i \overrightarrow{a_i} + \sum_{i=1}^{p} \frac{d}{dt} \left(\overrightarrow{[I_i]} \overrightarrow{\omega_i} \right)$$

where:

(F_{L5-S1}) are the net reaction forces;

n is the number of external forces;

F_j is the j-th external force (from the body acting on the environment else it should be +);

p is the number of body segments considered: 8 for the upper body model (hands, forearms, arms, head and trunk) and 7 for the lower body model (pelvis, thighs, shanks and feet);

$\vec{g} = \left[0, 0, -g\right]^t$ is the gravitational acceleration;

$\overrightarrow{r_j}$ is the position of the j-th external force;

r_{L5-S1} is the position of the L5-S1 joint;

r_i is the position of the centre of mass [42, 43] of the i-th segment;

m_i is the mass of the i-th segment;

a_i is the acceleration of the center of mass of the i-th segment;

I_i is the moment of inertia of the i-th segment;

ω_i is the angular velocity of the i-th segment.

The moments of inertia I_i can be calculated by modelling the overall system as follows: one cylinder for the trunk and head, two cylinders for the right and left upper arms, two cylinders for the right and left forearms and hands and one parallelepiped for the load. The formulas used for the calculation of the I_i are reported below:

$$I_i = \frac{1}{2} m_i \left(3\left(\frac{d_i}{2}\right)^2 + {h_i}^2 \right)$$

$$I_l = \frac{1}{12} m_l \left(d_l^2 + h_l^2 \right)$$

where:

m_i is the mass of the i-th segment;

h_i is the height of the i-th cylinder;

d_i is the diameter of the i-th cylinder;

m_l is the mass of the load;

h_l is the height of the parallelepiped;

d_l is the depth of the parallelepiped.

$\mathrm{F}_{\mathrm{L5-S1}}$ forces can be considered in a local reference system (LRS) on the trunk in which the y' axis is oriented as the vector C7-sacrum and $\mathrm{x}'\text{-}\mathrm{z}'$ represents the orthogonal plane to y'. In this LRS, the components of $\mathrm{F}_{\mathrm{L5-S1}}$ on the y' axis and the $\mathrm{x}'\text{-}\mathrm{z}'$ plane are called compression ($\mathrm{Fcompr}_{\mathrm{L5-S1}}$) and shear ($\mathrm{Fshear}_{\mathrm{L5-S1}}$) forces, respectively [43].

NOTE 1 In lifting tasks, these forces are correlated with risk levels [28], [30], [32] (Figure 14).

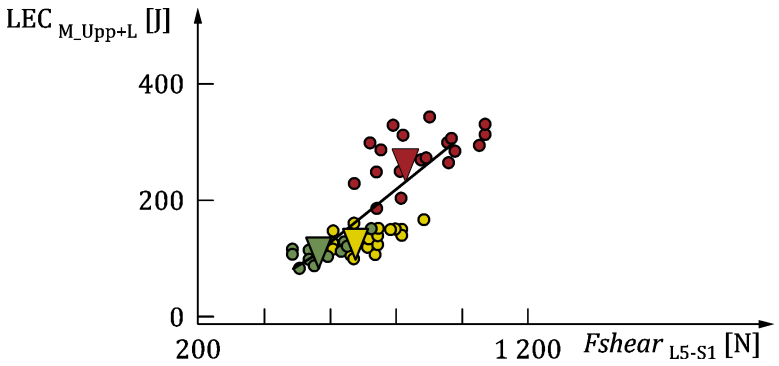

Key

LI = 1 LI = 2 LI = 3

Figure 14 — Correlation between the LEC_{M_Upp+L} and the maximum values of $Fshear_{L5-S1}$

The plot in Figure 14 contains 60 points, which correspond to the 20 subjects performing the three different lifting conditions (LI = 1, LI = 2 and LI = 3) in [30]. Triangles represent the mean of the twenty points for each lifting condition. The plot shows the r and p values. Bold type indicates statistical significance [30].

NOTE 2 To evaluate lumbosacral compression and shear forces at/in the spine, a kinematic/kinetic-based criterion has been used. The topic of estimating compressive and shear forces at the lumbosacral joint of the spine and their assessing with regard to biomechanical overload is very complex. In addition to "The Dortmund Lumbar Load Atlas", [44] which offers a comprehensive contribution on the objectification of lumbar load and lumbar load-bearing capacity during manual material handling, it is now possible to use appropriate musculoskeletal models that can also consider the contribution of muscle-generated forces to the overall force on L5-S1 joint. The estimation performed by these approaches will allow an even deeper understanding of the real stress on the spine. These methods use simple regression models based on the worker's muscle activity and trunk posture to estimate spinal compressions [45], [46] and optimization techniques [47], [48], [49], [50]. In addition, alternative approaches use sEMG signals to obtain data driven worker-specific musculoskeletal estimation [51], [52], [53].

8.3 Bipolar sEMG data

The sEMG signals can be processed as follows: the iMVC and the sEMG raw data of each lifting task are band-pass filtered using a fourth-order Butterworth filter of 20–400 Hz to reduce artifacts and other components of high-frequency noise [54], [55]. From these signals, the analysis of time and frequency domains can be performed. To extract the envelope of both iMVC and the sEMG signals of each lifting task, full-wave rectification, and low-pass filtering using a fourth-order Butterworth filter at 5 Hz are applied. For each muscle, the sEMG envelope is normalized to the average iMVC peak value [21], [56], [57]. From the elaborated sEMG signals of each lifting trial, in order to characterize differences in the sEMG activity between different conditions, the average rectified value (ARV), the root mean square (RMS) and the maximum value (Max) within the cycle can be calculated as follows:

$$ARV = \frac{1}{101}\sum_{k=0}^{100} sEMG_k$$

$$RMS = \sqrt{\frac{1}{101}\sum_{k=0}^{100} sEMG_k^2}$$

$$Max = max_{k=0,\ldots,100}\left(sEMG_k\right)$$

The co-activation of the trunk muscles can be computed by considering the time-varying multi-muscle co-activation function (TMCf) proposed by Ranavolo and colleagues [31]:

$$TMCf\left(d\left(k\right),k\right) = \left(1 - \frac{1}{1+e^{-12\left(d\left(k\right)-0.5\right)}}\right).\frac{\left(\sum_{m=1}^{M} sEMG_m\left(k\right)/\left(M\right)\right)^2}{max_{m=1\ldots M}\left[sEMG_m\left(k\right)\right]}$$

where:

TMCf is the time-varying multi-muscle co-activation function;

$d\left(k\right)$ is the mean of the differences between each pair of $\mathrm{sEMG_m}\left(k\right)$;

M is the number of muscles considered in the analysis;

$sEMG_m$ is the sEMG signal of the m-th muscle;

$\mathrm{sEMG_m}\left(k\right)$ given by the following formula:

$$d\left(k\right) = \left(\frac{\sum_{m=1}^{M-1}\sum_{n=m+1}^{M}\left|EMG_m\left(k\right) - EMG_n\left(k\right)\right|}{Lx\left(M!/\left(2!\left(M-2\right)!\right)\right)}\right)$$

where:

$sEMG_n$ is the sEMG signal of the n-th muscle;

L is the length of the sEMG signal.

As co-activation indices, the area of total TMCf (TMCfArea) and the max value (TMCfMax) within the cycles can be used [28], [31].

Using the band-pass filtered sEMG data, the power spectral density can be estimated using Yule-Walker's approach on the signal portion recorded during the detected tasks: the autoregressive parameters can be estimated using Levinson Durbin recursion with a model order p = 15 [6]. For each muscle, the mean frequency (MNF) and the median frequency (MDF) can be computed and they are normalized to the MNF and MDF calculated from the iMVC spectra, respectively.

NOTE During lifting tasks, these indexes are related to risk levels [6], [28].

EXAMPLE Figure 15 shows surface electromyographic ARV (means and standard deviations) of 20 subjects of the bilateral trunk muscles (erector spinae longissimus-ESL, erector spinae iliocostalis-ESI, multifidus-M, latissimus

dorsi-LD, rectus abdominis superior-RAS and rectus abdominis middle-RAM), while performing manual lifting tasks at three different risk condition with three lifting index (LI = 1, 2 and 3). The asterisks in the figure show the significant differences at statistical analysis between the pairs of LI [28].

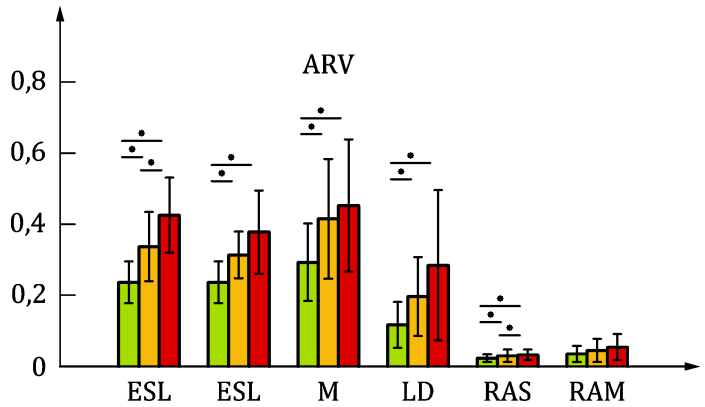

Key

LI = 1 *LI = 2* *LI = 3*

ESL	erector spinae longissimus
ESI	erector spinae iliocostalis
M	multifidus
LD	latissimus dorsi
RAS	rectus abdominis superior
RAM	rectus abdominis middle
*	significant differences at statistical analysis [28]

Figure 15 — Surface electromyographic average rectified value (ARV) of the trunk muscles

8.4 High Density sEMG data

HDsEMG signals can be digitally band-pass filtered in the frequency bandwidth 20–400 Hz (3rd order Butterworth filter) and the bipolar EMG signals can be obtained from the grid.

EXAMPLE 1 If the signals are acquired by using HDsEMG via 64-channel grids consisting of 13 rows and five columns of electrodes with one electrode absent from the upper corner [58], [59], 59 bipolar EMG signals can be obtained from each grid (12 longitudinal bipolar recordings in each column except the first column of the grid, which had 11 electrode pairs) by subtracting the signals from two adjacent electrodes along the fibers direction [60].

To characterize the spatial distribution of muscle activity, the following variables can be extracted from each of bipolar recordings [49], [50]:

— the mean root mean square (RMS) across the grid (RMSfull_grid) by averaging the RMSs for each bipolar signal;

— the RMS of the region of activation (RoA, RMSRoA) via the mean RMS for the area of each of the four neighbouring electrodes. The RoA was considered as the area with the highest mean RMS [34];

— the correlation coefficients between the RMS values of each bipolar signal in each cycle and the RMS values of the first cycle (CorrCoeffRMS) [61];

— the coefficient of variation (CV) of both coordinates (CVGx and CVGy) of the center of gravity (G). Such coefficient assesses the variability of the center of gravity during the lifting task. The two coordinates of G represent the point where the 59 RMS values are concentrated on average of the RMS map [50], [62], [63], [64] and can be evaluated as follows:

$$G_x = \frac{1}{RMS_{total}} \sum_{i=1}^{59} RMS_i x_i$$

$$G_y = \frac{1}{RMS_{total}} \sum_{i=1}^{59} RMS_i y_i$$

where:

G_x is the medio-lateral direction;

G_y is the cranial–caudal direction;

RMS_{total} is the sum of the RMS values across the grid;

RMS_i is the RMS value at the i-th position of the corresponding coordinates (x_i, y_i).

The topographical map of acquired muscle (Figure 16) activity can be created using the RMS values for each bipolar signal.

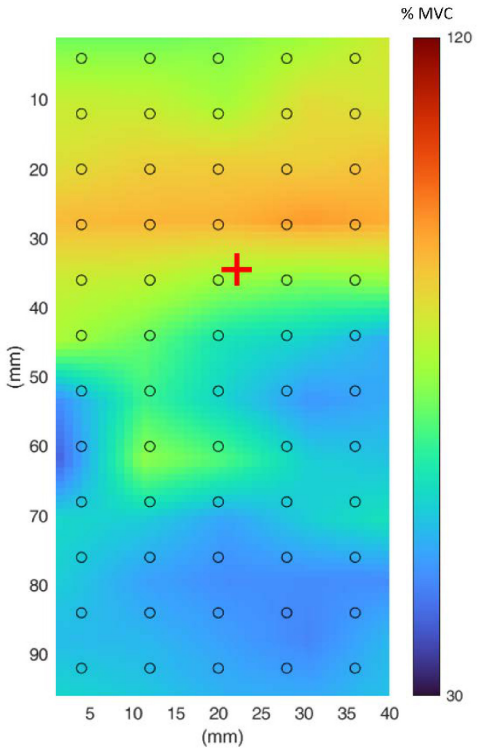

Figure 16 — Map of acquired muscle activity detected by using HDsEMG

EXAMPLE 2 Potvin Method

Ergonomists and engineers adopt Potvin's approach, [36], [37], [65], to quantify physical effort in repetitive tasks. To enable the assessment of repetitive force and torque limits, this method provides a Threshold Limit Value (TLV®[12]) fatigue curve that can be used to compute acceptable percent duty cycle (DC, percent of time over a work cycle or a certain time period that forces is applied) for a given force (% Maximum Voluntary Contraction, MVC) or an acceptable % MVC for a given percent duty cycle, according to the following formula:

$$DC = 100*\left(exp\left(0.066 - \left(\left(MVC \,/\, 100\right) / 0.143\right)\right)\right)$$

The TLV® applies to duty cycle within the range 0.5% to 90%. The TLV® is intended for cyclical work normally performed for 2 or more hours per day. The TLV is intended for healthy workers. If a worker does multiple tasks that are each 2 hours or more, none of the tasks should exceed the TLV®. Static exertions of the hand, elbow or shoulder would not be expected to exceed 20 minutes (Figure 17).

NOTE The ACGIH refitted Potvin's data so the TLV curve presented in the ACGIH TLVs and BEIs is not identical to Potvin's original work.

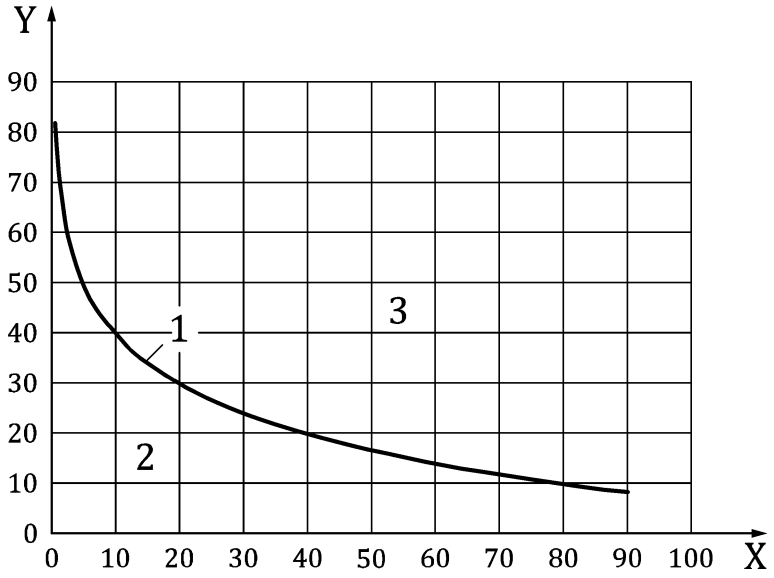

Key

1	TLV©	X	%DC
2	acceptable	Y	%MVC
3	not accectable		

Figure 17 — ACGIH. TLVs [36], [37], [65]

EXAMPLE 3 Joint Analysis of EMG Spectrum and Amplitude (JASA) Method

Joint Analysis of EMG Spectrum and Amplitude (JASA) was introduced [38], [66] to considerate the simultaneous changes in the EMG amplitude and spectrum. For this purpose, the behaviour of the EMG amplitude (i.e. RMS) and spectrum (i.e. Median Frequency) over time of EMG recording is studied performing linear regression analyses (Figure 18). Such an analysis results for each recording in a pair of values characterised by the slope of the RMS and MDF regression lines. Such a pair of values can be graphically presented by a dot in the 'JASA plot' shown in Figure 17. In this xy diagram changes in the EMG are classified according to the position of the dot within the four quadrants of the diagram into four

[12] Threshold Limit Value (TLV®) is an example of a suitable product available commercially. This information is given for the convenience of users of this document and does not constitute an endorsement by CEN of this product.

categories as ‘fatigue’, ‘recovery’, ‘force increase’, or ‘force decrease’. This classification is based on known relationships between characteristics of the EMG amplitude (RMS) and spectral parameters (MDF) on force and fatigue. The dependency of both EMG indicators on the fatigue state and the force production has been studied in numerous investigations: regarding the EMG amplitude, it is experimentally verified that the amplitude increases with increasing force as well as with the occurrence with fatigue [29]. For the spectral distribution, a shift to lower frequencies with fatigue and a shift to higher ones with increasing force was reported [38]. The interpretation of the causes for the EMG changes presented in four quadrants of Figure 18 are based on the concordant statements which can be drawn from the joint consideration of the respective changes in the EMG amplitude and spectrum. Accordingly, dots in the lower right-hand quadrant are characterised as caused by ‘fatigue’, since both, the increase in RMS and the decrease in MF indicate fatigue. Similarly, dots in the other three quadrants are classified as ‘force increase’, ‘force decrease’, and ‘recovery’ since—depending on the location of the dot within the co-ordinate system—both indicators point to one of these statements [38].

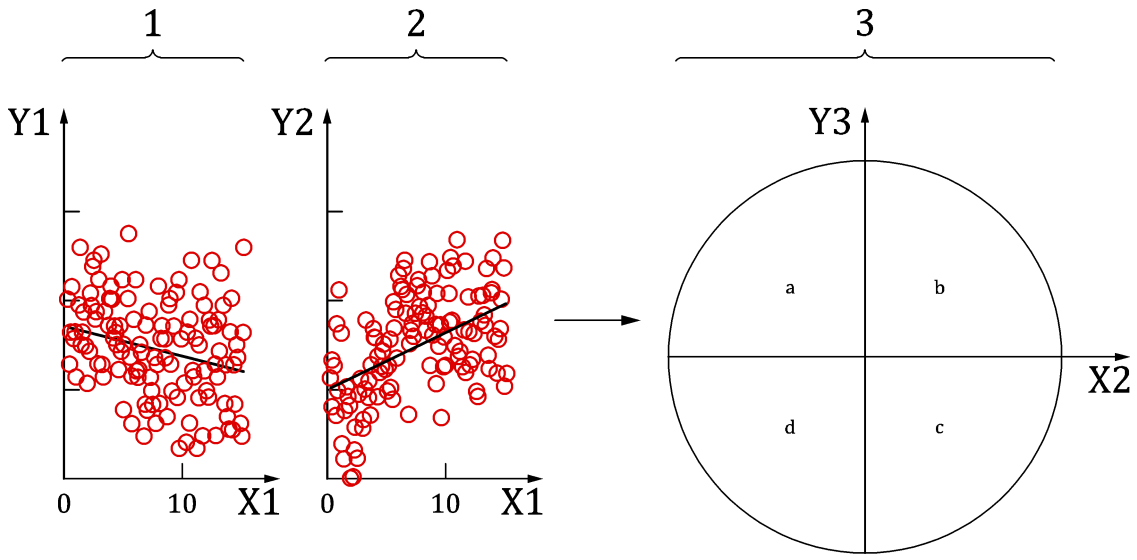

Key

1	Fmedian	X2	amplitude slope	a	recovery
2	RMS	Y1	Hz	b	force increase
3	JASA	Y2	% MVC	c	fatigue
X1	Time [min]	Y3	frequency slope	d	force decrease

Figure 18 — Example of joint Analysis of EMG Spectrum and Amplitude (JASA).

9 Machine learning algorithms for risk classification

ANNs can be used to estimate the biomechanical risk in terms of LI based on pre-processed kinematic features, kinetic and sEMG data as schematically described in Figure 19.

NOTE Particularly, in Figure 19 a set of feedforwards ANNs trained using different feature combinations and different network topologies is reported.

The latter can be implemented by varying the number of Hidden Layers (HL) and the number of Neurons (N) populating each HL. The output set (OS) provided an orthogonal coding of the three LI levels: (1 0 0), (0 1 0) and (0 0 1) representing LI = 1, LI = 2 and LI = 3, respectively. Different features can be combined into different training sets constituted combining the kinematic, kinetic and sEMG features in different ways. In terms of network architecture, different network architectures defined by the combination of number of HL and number of N in each layer can be tested. A Levenberg-Marquardt back-propagation

algorithm [67] can be used to train the ANNs; the stopping criterion can be defined as the occurrence of at least one of the following conditions: number of iterations = 1000, number of consecutive fails on the validation set = 6, mean square error < 10^{-6} [10], [11]. Different ANNs can be trained combing different network topologies and different training sets using for each training a random set of 80 % samples as the training test, 10% as the validation test and 10 % as the testing set. A confusion matrix 3 × 3 can be calculated for each ANNs considering the actual LI and the one estimated by the ANN on the randomly extracted testing set. Then, the mean confusion matrix can be obtained for each network topology and each set. A performance parameter (P) can be calculated as the mean (%) of the elements on the diagonal of these confusion matrices, where 100% indicates the absence of misclassifications [5], [6].

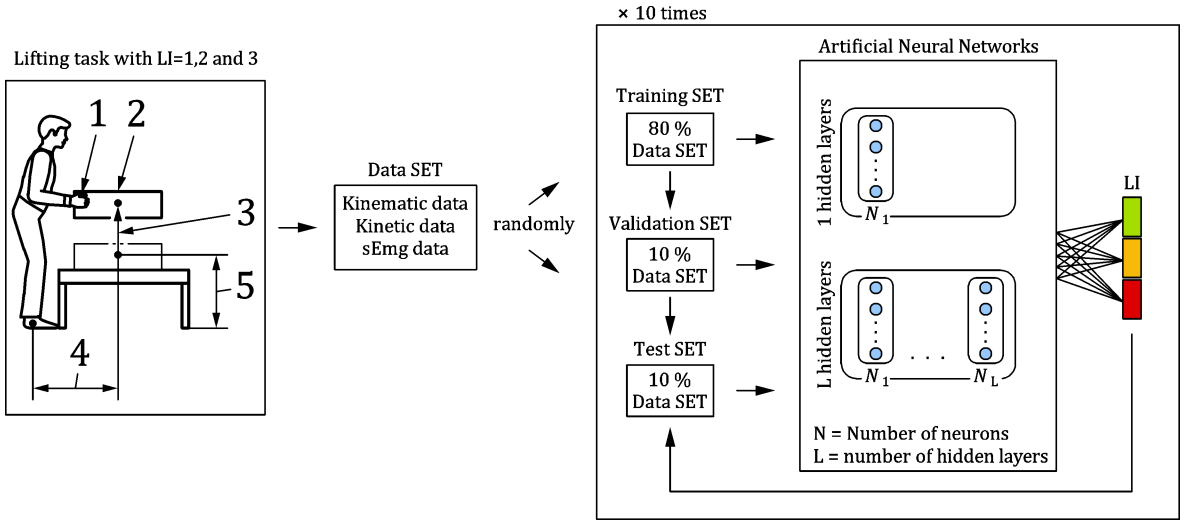

Key

1	good hand-to-object coupling	3	vertical travel distance	LI = 1
2	object center of mass	4	horizontal location	LI = 2
5	vertical location			LI = 3

Figure 19 — Schematic diagram of Machine Learning approach

The three boxes of the flowchart in Figure 19 represent the lifting task, the feature extraction from recorded data, and the ANN architecture to map kinetic features on the Lifting Index (1, 2, and 3) levels [5], [6].

Annex A
(informative)

Rating the RNLE method by measuring all the task variables through the use of IMUs

The use of IMUs allows the real-time automatic estimation of the task variables needed for the rating of the RNLE multipliers as follows:

$$LI = \frac{L}{RWL(Start)} = \frac{L}{LC \cdot HM(Start) \cdot VM(Start) \cdot DM_{SS} \cdot AM_{SS} \cdot FM_{SS} \cdot CM}$$

where:

LI is the Lifting Index;

L is the actual weight of the lifted load;

RWL is the recommended weight limit (RWL) calculated for the task;

LC is the constant load of 23 kg;

CM is the coupling multiplier for the quality of gripping.

HM is evaluated as follows:

$$HM(Start) = \frac{0,25}{H(Start)} = \frac{0,25}{Hands_{mp}(Start) - Foot_{p}(Start)}$$

$Hands_{mp}$ is the middle point of the hands;

$Foot_{p}$ is the middle point of the feet;

H is the distance between $Hands_{mp}$ and $Foot_{p}$ at the beginning of the lifting (Start);

HM is the horizontal distance multiplier derived by measuring the horizontal distance H.

VM is evaluated as follows:

$$VM(Start) = 1 - 0,3 \cdot \left| 0,75 - V\left(Start\right) \right|$$

VM is the vertical multiplier derived by measuring the vertical location of the load V.

DM is evaluated as follows:

$$DM_{SS} = 0,82 + \frac{0,045}{D_{SS}} = 0,82 + \frac{0,045}{V\left(Stop\right) - V\left(Start\right)}$$

DM is the vertical displacement multiplier derived by measuring the vertical displacement of the load D;

D is the differences among the vertical location of the load at the end (stop) and at the beginning of the lifting (Start).

AM is evaluated as follows:

$$AM_{SS} = 1\text{-}0{,}0032 \cdot A_{SS} = 1\text{-}0{,}0032 \cdot [\,A(\mathrm{Stop}) - A(\mathrm{Start})]$$

AM is the asymmetry multiplier derived by measuring the trunk angle of asymmetry A.

FM is evaluated as follows:

$$FM(i) = f(F(i)) = f\left(\frac{n_{lifts}(i)}{\min}\right)$$

FM is the frequency multiplier depending on lifting frequency (F, numbers of lifting (n_{lifts})/min), lifting duration and vertical location.

Annex B
(informative)

Indexes for the biomechanical risk assessment

Indeed, several potential instrumental-based assessment techniques have been developed in earlier investigations [2], [3]. These quantitative methods rely on computing kinematic, kinetic, and surface electromyography (sEMG)-based indices like mechanical lifting energy consumption [30], compression and shear forces at the first sacral and fifth lumbar vertebrae of the spine [28], and trunk muscle activation and co-activation [28], [32]. These indices are sensitive to different lifting risk conditions and have a positive correlation with the physical factors that put stress on the spine's sacral-lumbar area (i.e. compressive and shear forces in that region). The cost of computing indices is very low, and unobtrusive, wireless, wearable, miniaturized, and low power consumption sensors can be used to record data from the human body [2], [3].

Inertial measurement units (IMUs), wireless shoe insoles for measuring ground reaction force, and bipolar sEMG probes are the most frequently utilized systems [2], [3]. Artificial neural networks (ANNs), which perform well when adequate kinematic and sEMG datasets are selected [5], [6], are used to optimize instrumental-based methods for biomechanical risk classification [5], [6].

Varrecchia et al. [5], [6] carried out numerous acquisitions at the Ergonomics and Physiology Laboratory of the Department of Medicine, Epidemiology, Occupational and Environmental Hygiene of INAIL in Monte Porzio Catone (Rome, Italy), where the kinematic, kinetic, and sEMG data were acquired to define which indexes import in the tool and to enhance the knowledge of biomechanical indexes connected with the biomechanical risk during the execution of various MMH activities. And the execution of these experimental sessions was possible thanks to the local ethics committee’s consent (N. 0078009/2021).

Bibliography

[1] Ranavalo, A., Ajoudani, A., Cherubini, A., Bianchi, M., Fritzsche, L., Iavicoli, S., Sartori, M., Silvetti, A., Vanderborght, B., Varrecchia, T., Draicchio, F. The Sensor-Based Biomechanical Risk Assessment at the Base of the Need for Revising of Standards for Human Ergonomics. Sensors (Basel). 2020, 20(20):5750 [viewed 2023-08-03]. Available at: https://doi.org/10.3390/s20205750

[2] Alberto, R., Draicchio, F., Varrecchia, T., Silvetti, A., Iavicoli, S. Wearable Monitoring Devices for Biomechanical Risk Assessment at Work: Current Status and Future Challenges—A Systematic Review. Int. J. Environ. Res. Public Health 2018, 15(11), 2001; Erratum in 2018, 15(11):2569 [viewed 2023-08-03]. Available at: https://doi.org/10.3390/ijerph15112569

[3] Ranavolo, A., Draicchio, F., Varrecchia, T., Silvetti, A., Iavicoli, S. Erratum: Alberto, R. Wearable Monitoring Devices for Biomechanical Risk Assessment at Work: Current Status and Future Challenges—A Systematic Review. Int. J. Environ. Res. Public Health 2018, 15(11):2569 [viewed 2023-08-03]. Available at: https://doi.org/10.3390/ijerph15112569

[4] Kim, W., Garate V.R., Gandarias, J., Lorenzini, M., Ajoudani, A. A Directional Vibrotactile Feedback Interface for Ergonomic Postural Adjustment. IEEE Trans Haptics. 2022, 15(1), 200-211 [viewed 2023-08-03]. Available at: 10.1109/TOH.2021.3112795

[5] Varrecchia, T., De Marchis, C., Draicchio, F., Schmid, M., Conforto, S., Ranavolo, A. Lifting Activity Assessment Using Kinematic Features and Neural Networks. Appl. Sci, 2020, 10(6), 1989 [viewed 2023-08-03]. Available at: https://doi.org/10.3390/app10061989

[6] Varrecchia, T., De Marchis, C., Rinaldi, M., Draicchio, F., Serrao, M., Schmid, M., Conforto, S., Ranavolo, A. Lifting Activity Assessment Using Surface Electromyographic Features and Neural Networks. International Journal of Industrial Ergonomics. 2018, 66, 1-9 [viewed 2023-08-03]. Available at: https://doi.org/10.1016/j.ergon.2018.02.003

[7] Ajoudani, A., Albrecht, P., Bianchi, M., Cherubini, A., Del Ferraro, S., Fraisse, P., Fritzsche, L., Garabini, M., Ranavolo, A., Rosen, P.H., Sartori, M., Tsagarakis, N., Vanderborght, B., Wischniewski, S. Smart Collaborative Systems for Enabling Flexible and Ergonomic Work Practices [Industry Activities]. IEEE Robotics & Automation Magazine. 2020, 27(2), 169-176 [viewed 2023-08-03]. Available at: 10.1109/MRA.2020.2985344

[8] Bernard, B.P., Musculoskeletal Disorders and Workplace Factors: A Critical Review of Epidemiologic Evidence for Work-Related Musculoskeletal Disorders of the Neck, Upper Extremity, and Lower Back. DHHS (NIOSH) Publication, 1997, 97-141. Washington, DC, USA. [viewed 2023-08-03] Available at: https://stacks.cdc.gov/view/cdc/21745

[9] Bao, S., Howard, N., Lin, J.-H. Are work-related Musculoskeletal Disorders Claims Related to Risk Factors in Workplaces of the Manufacturing Industry? Ann. Work. Expo. Heal. 2020, 64, 152–164 [viewed 2023-08-03]. Available at: 10.1093/annweh/wxz084

[10] Shalev-Shwartz, S., and Ben-David, S. Understanding Machine Learning. 2014. Published 2014 by Cambridge University Press [viewed 2023-08-03]. Available at: https://www.cs.huji.ac.il/~shais/UnderstandingMachineLearning/

[11] Picerno, P., Iosa, M., D'Souza, C., Benedetti, M.G., Paolucci, S., Morone, G. Wearable Inertial Sensors for Human Movement Analysis: A Five-year Update. Expert Rev Med Devices. 2021, 18(sup1), 79-94 [viewed 2023-08-03]. Available at: 10.1080/17434440.2021.1988849

[12] Prasanth, H., Caban, M., Keller, U., Courtine, G., Ijspeert, A., Vallery, H., von Zitzewitz, J. Wearable Sensor-Based Real-Time Gait Detection: A Systematic Review. Sensors (Basel). 2021, 21(8):2727 [viewed 2023-08-03]. Available at: https://doi.org/10.3390/s21082727

[13] Faisal ,A.I., Majumder, S., Mondal, T., Cowan, D., Naseh, S., Deen, M.J. Monitoring Methods of Human Body Joints: State-of-the-Art and Research Challenges. Sensors (Basel). 2019, 19(11):2629 [viewed 2023-08-03]. Available at: https://doi.org/10.3390/s19112629

[14] Shahabpoor, E., Pavic, A. Measurement of Walking Ground Reactions in Real-Life Environments: A Systematic Review of Techniques and Technologies. Sensors (Basel). 2017, 17(9):2085 [viewed 2023-08-03]. Available at: https://doi.org/10.3390/s17092085

[15] The Institute of Electricaland Electronics Engineers, Inc. Surface Electromyography. Physiology, engineering and applications. IEEE Press, J. Wiley, Edited by Merletti, R., and Farina, D. 2016 [viewed 2023-08-03]. Available at: https://onlinelibrary.wiley.com/doi/book/10.1002/9781119082934

[16] Nova Biomedical. Surface Electromyography. Fundamentals, computational techniques and clinical applications. Nova Science Publishers Inc. Edited by Mitchell, D. 2016. ISBN: 978-1-53610-202-4

[17] Institute of Electrical and Electronics Engineers. Electromyography. Physiology, Engineering, and Noninvasive Applications. IEEE Press, J. Wiley, Edited by Merletti R and Parker PA. 2004. ISBN:9780471675808

[18] Edizioni Universitarie Romane. Principi di Elettromiografia di Superficie. Edited by Ranavolo, A. 2021. ISBN 976-88-6022-396-8

[19] Merletti, R. Non Invasive Electromyography. [viewed 2023-06-14]. Available at: https://www.robertomerletti.it

[20] Hermens, H.J., Freriks, B., Merletti, R., Stegeman, D., Blok, J., Rau, G., Disselhorst-Klug, C., Hagg, G. European recommendations for surface electromyography. 8th Deliverable of the SENIAM Project. 1999. ISBN 90-75452-15-2

[21] Barbero, M., Merletti, R., Rainoldi, A.. Atlas of Muscle Innervation Zones: Understanding Surface Electromyography and its Applications. Springer, New York. 2012 [viewed 2023-08-03]. Available at: https://doi.org/10.1007/978-88-470-2463-2

[22] Ringelberg, J.A. EMG and force production of some human shoulder muscles during isometric abduction. Journal of Biomechanics, 1985, 18(12), 939-947 [viewed 2023-08-03]. Available at: 10.1016/0021-9290(85)90037-5

[23] Muller, A., Mecheri, H., Corbeil, P., Plamondon, A., Robert-Lachaine, X. Inertial Motion Capture-Based Estimation of L5/S1 Moments during Manual Materials Handling. Sensors (Basel). 2022, 22(17):6454 [viewed 2023-08-03] Available at: https://doi.org/10.3390/s22176454

[24] Donisi, L., Cesarelli, G., Pisani, N., Ponsiglione, A.M., Ricciardi, C., Capodaglio, E. Wearable Sensors and Artificial Intelligence for Physical Ergonomics: A Systematic Review of Literature.

Diagnostics (Basel). 2022, 12(12):3048 [viewed 2023-08-03]. Available at: https://doi.org/10.3390/diagnostics12123048

[25] Rattanakoch, J., Samala, M., Limroongreungrat, W., Guerra, G., Tharawadeepimuk, K., Nanbancha, A., Niamsang, W., Kerdsomnuek, P., Suwanmana, S. Validity and Reliability of Inertial Measurement Unit (IMU)-Derived 3D Joint Kinematics in Persons Wearing Transtibial Prosthesis. Sensors (Basel). 2023, 23(3):1738 [viewed 2023-08-03]. Available at: https://doi.org/10.3390/s23031738

[26] Riek, P.M., Best, A.N., Wu, A.R. Validation of Inertial Sensors to Evaluate Gait Stability. Sensors (Basel). 2023, 23(3):1547 [viewed 2023-08-03]. Available at: https://doi.org/10.3390/s23031547

[27] Perotto, A.O. Anatomical guide for the electromyographer: the limbs and trunk. Charles C Thomas Publisher. 2011

[28] Ranavolo, A., Varrecchia, T., Iavicoli, S., Marchesi, A., Rinaldi, M., Serrao, M., Conforto, S., Cesarelli, M., Draicchio, F. Surface electromyography for risk assessment in work activities designed using the “revised NIOSH lifting equation”. International Journal of Industrial Ergonomics. 2018, 68:34-45 [viewed 2023-08-03]. Available at: doi: https://doi.org/10.1016/j.ergon.2018.06.003

[29] Ranavolo, A., Chini, G., Silvetti, A., Mari, S., Serrao, M., Draicchio, F. Myoelectric manifestation of muscle fatigue in repetitive work detected by means of miniaturized sEMG sensors. Int J Occup Saf Ergon. 2018, 24(3):464-474 [viewed 2023-08-03]. Available at: https://doi.org/10.1080/10803548.2017.1357867

[30] Ranavolo, A., Varrecchia, T., Rinaldi, M., Silvetti, A., Serrao, M., Conforto, S., Draicchio, F. Mechanical lifting energy consumption in work activities designed by means of the "revised NIOSH lifting equation". Ind Health. 2017, 55(5):444-454 [viewed 2023-08-03]. Available at: 10.2486/indhealth.2017-0075

[31] Ranavolo, A., Mari, S., Conte, C., Serrao, M., Silvetti, A., Iavicoli, S., Draicchio, F. A New Muscle Co-activation Index For Biomechanical Load Evaluation in Work Activities. Ergonomics. 2015, 58(6):966-79 [viewed 2023-08-03]. Available at: 10.1080/00140139.2014.991764

[32] Chini, G., Varrecchia, T., Tatarelli, A., Silvetti, A., Fiori, L., Draicchio, F., Ranavolo, A. Trunk Muscle Co-activation and Activity in One- and Two-person Lifting. International Journal of Industrial Ergonomics, 2022, 89 [viewed 2023-08-03]. Available at: https://doi.org/10.1016/j.ergon.2022.103297

[33] Varrecchia, T., Conforto, S., De Nunzio, A.M., Draicchio, F., Falla, D., Ranavolo, A. Trunk Muscle Coactivation in People with and without Low Back Pain during Fatiguing Frequency-Dependent Lifting Activities. Sensors 2022, 22(4), 1417 [viewed 2023-08-03]. Available at: https://doi.org/10.3390/s22041417

[34] Varrecchia, T., Ranavolo, A., Conforto, S., De Nunzio, A.M., Arvanitidis, M., Draicchio, F., Falla, D. Bipolar versus High-density Surface Electromyography for Evaluating Risk in Fatiguing Frequency-dependent Lifting Activities. Appl Ergon. 2021, 95:103456 [viewed 2023-08-03]. Available at: https://doi.org/10.1016/j.apergo.2021.103456

[35] D'Anna, C., Varrecchia, T., Ranavolo, A., De Nunzio, A.M., Falla, D., Draicchio, F., Conforto, S. Centre of Pressure Parameters For the Assessment of Biomechanical Risk in Fatiguing Frequency-dependent Lifting Activities. PLoS One. 2022, 17(8) [viewed 2023-08-03]. Available at: 10.1371/journal.pone.0266731

[36] Potvin, J.R. An equation to predict maximum acceptable loads for repetitive tasks based on duty cycle: evaluation with lifting and lowering tasks. Work. 2012, 41(Supplement 1), 397-400 [viewed 2023-08-03]. Available at: 10.3233/WOR-2012-0189-397

[37] Potvin, J.R. Predicting maximum acceptable efforts for repetitive tasks: an equation based on duty cycle. Human factors. 2012, 54(2), 175-188 [viewed 2023-08-03]. Available at: 10.1177/0018720811424269

[38] Hägg, G.M., Luttmann, A., Jäger, M. Methodologies for evaluating electromyographic field data in ergonomics. Journal of electromyography and kinesiology. 2000 10(5), 301-312 [viewed 2023-08-03]. Available at: https://doi.org/10.1016/S1050-6411(00)00022-5

[39] Fazio, P., Granieri, G., Casetta, I., Cesnik, E., Mazzacane, S., Caliandro, P., Pedrielli, F., and Granieri, E. Gait Measures with a Triaxial Accelerometer among Patients with Neurological Impairment. Neurological Sciences. 2013, 34(4), 435-440 [viewed 2023-08-03]. Available at: 10.1007/s10072-012-1017-x

[40] Sakata, K., Kogure, A., Hosoda, M., Isozaki, K., Masuda, T., and Morita, S. Evaluation of the Age-related Changes in Movement Smoothness in the Lower Extremity Joints During Lifting. Gait & posture. 2010, 31(1), 27-31 [viewed 2023-08-03]. doi: https://doi.org/10.1016/j.gaitpost.2009.08.239

[41] Zatsiorsky, V.M., Seluyanov, V.N., Chugunova, L.G. Methods of Determining Massinertial Characteristics of the Main Segments of the Human Body. Biomechanics VIII-B, Edited by Matsui, H. and Kobayashi, K., 1990. Human Kinetic, Illinois, 1152-1159.

[42] de Leva, P. Adjustments to Zatsiorsky-Seluyanov'ssegment Inertia Parameters. J Biomech. 1996, 29(9), 1223– 30 [viewed 2023-08-03]. Available at: 10.1016/0021-9290(95)00178-6

[43] Plamondon, A., Gagnon, M., Desjardins, P. Validation of two 3-D Segment Models to Calculate the Net Reaction Forces and Moments at the L5S1 Joint in Lifting. Clinical Biomechanics. 1996, 11(2) [viewed 2023-08-03]. Available at: https://doi.org/10.1016/0268-0033(95)00043-7

[44] Jäger, M. The Dortmund Lumbar Load Atlas. A Contribution to Objectifying Lumbar Load and Load-Bearing Capacity for an Ergonomic Work Design of Manual Materials Handling. 2023

[45] Arjmand, N., Plamondon, A., Shirazi-Adl, A., Larivière, C., Parnianpour, M. Predictive Equations to Estimate Spinal Loads in Symmetric Lifting Tasks. J. Biomech. 2011, 44, 84–91 [viewed 2023-08-03]. Available at: https://doi.org/10.1016/j.jbiomech.2010.08.028

[46] Mientjes, M.I.V., Norman, R.W., Wells, R.P., Mcgill, S.M. Assessment of an EMG-based Method for Continuous Estimates of Low Back Compression During Asymmetrical Occupational Tasks. Ergonomics. 1999, 42, 868–879 [viewed 2023-08-03]. Available at: https://doi.org/10.1080/001401399185342

[47] Bazrgari, B., Shirazi-Adl, A., Arjmand, N. Analysis of Squat and Stoop Dynamic Liftings: Muscle Forces and Internal Spinal Loads. Eur. Spine J. 2007, 16, 687–699 [viewed 2023-08-03]. Available at: https://doi.org/10.1007/s00586-006-0240-7

[48] Cholewicki, J., McGill, S.M., Norman, R.W. Comparison of Muscle Forces and Joint Load From an Optimization and EMG Assisted Lumbar Spine Model: Towards Development of a Hybrid Approach. J. Biomech. 1995, 28 [viewed 2023-08-03]. Available at: https://doi.org/10.1016/0021-9290(94)00065-C

[49] Kim, H.K., Zhang, Y. Estimation of Lumbar Spinal Loading and Trunk Muscle Forces During Asymmetric Lifting Tasks: Application of Whole-body Musculoskeletal Modelling in OpenSim. Ergonomics. 2017, 60, 563–576 [viewed 2023-08-03]. Available at: https://doi.org/10.1080/00140139.2016.1191679

[50] von Arx, M., Liechti, M., Connolly, L., Bangerter, C., Meier, M.L., Schmid, S. From Stoop to Squat: A Comprehensive Analysis of Lumbar Loading Among Different Lifting Styles. Front. Bioeng. Biotechnol. 2021, 9, 1–13 [viewed 2023-08-03]. Available at: https://doi.org/10.3389/fbioe.2021.769117

[51] Lloyd, D.G., Besier, T.F. An EMG-driven Musculoskeletal Model to Estimate Muscle Forces and Knee Joint Moments in Vivo. J. Biomech. 2003, 36, 765–7760 [viewed 2023-08-03]. Available at: https://doi.org/10.1016/S0021-9290(03)00010-1

[52] Moya-Esteban, A., van der Kooij, H., Sartori, M., Robust Estimation of Lumbar Joint Forces in Symmetric and Asymmetric Lifting Tasks via Large-scale Electromyography-driven Musculoskeletal Models. J. Biomech. 2022a, 144, 111307 [viewed 2023-08-03]. Available at: https://doi.org/10.1016/j.jbiomech.2022.111307

[53] Sartori, M., Reggiani, M., Farina, D., Lloyd, D.G. EMG-Driven Forward-Dynamic Estimation of Muscle Force and Joint Moment about Multiple Degrees of Freedom in the Human Lower Extremity. PLoS One. 2012, 7(12) [viewed 2023-08-03]. Available at: https://doi.org/10.1371/journal.pone.0052618

[54] Butler, H.L., Newell, R., Hubley-Kozey, C.L., Kozey, J.W. The Interpretation of Abdominal Wall Muscle Recruitment Strategies Change When the Electrocardiogram (ECG) is Removed from the Electromyogram (EMG). Journal of Electromyography and Kinesiology. 2009, 19(2), e102-e113 [viewed 2023-08-03]. Available at: 10.1016/j.jelekin.2007.10.004

[55] Drake, J.D., Callaghan, J.P. Elimination of Electrocardiogram Contamination from Electromyogram Signals: An Evaluation of Currently Used Removal Techniques. J. Electromyogr. Kinesiol. 2006, 16(2), 175–187 [viewed 2023-08-03]. Available at: 10.1016/j.jelekin.2005.07.003

[56] Marras, W.S., and Davis, K.G. A non-MVC EMG Normalization Technique for the Trunk Musculature: Part 1. Method Development. Journal of electromyography and kinesiology, 2001, 11(1), 1-9 [viewed 2023-08-03]. Available at: https://doi.org/10.1016/S1050-6411(00)00039-0

[57] Burden, A. How Should We Normalize Electromyograms Obtained From Healthy Participants? What We Have Learned from Over 25 Years of Research. Journal of electromyography and kinesiology. 2010, 20(6), 1023-1035 [viewed 2023-08-03]. Available at: 10.1016/j.jelekin.2010.07.004

[58] Farina, D., Leclerc, F., Arendt-Nielsen, L., Buttelli, O., Madeleine, P. The Change in Spatial Distribution of Upper Trapezius Muscle Activity is Correlated to Contraction Duration. J. Electromyogr. Kinesiol. 2008, 18(1), 16–25 [viewed 2023-08-03]. Available at: 10.1016/j.jelekin.2006.08.005

[59] Falla, D., Gizzi, L., Tschapek, M., Erlenwein, J., Petzke, F. Reduced Task-induced Variations in the Distribution of Activity Across Back Muscle Regions in Individuals with Low Back Pain. Pain. 2014, 155, 944–953 [viewed 2023-08-03]. Available at: 10.1016/j.pain.2014.01.027

[60] Stegeman, D.F., Kleine, B.U., Lapatki, B.G., Van Dijk, J.P. High-density Surface EMG: Techniques and Applications at a Motor Unit Level. Biocybern. Biomed. Eng. 2012, 32(3), 3–27 [viewed 2023-08-03]. Available at: https://doi.org/10.1016/S0208-5216(12)70039-6

[61] Watanabe, K., Kouzaki, M., Merletti, R., Fujibayashi, M., & Moritani, T. Spatial EMG Potential Distribution Pattern of Vastus Lateralis Muscle During Isometric Knee Extension in Young and Elderly Men. J Electromyogr Kinesiol. 2012, 22(1), 74-79 [viewed 2023-08-03]. Available at: https://doi.org/10.1016/j.jelekin.2011.09.010

[62] Falla, D., Cescon, C., Lindstroem, R., Barbero, M., X. Muscle Pain Induces a Shift of the Spatial Distribution of Upper Trapezius Muscle Activity During a Repetitive Task: A Mechanism for Perpetuation of Pain with Repetitive Activity? Clin. J. Pain. 2017, 33, 1006–1013 [viewed 2023-08-03]. Available at: 10.1097/AJP.0000000000000513

[63] Madeleine, P., Leclerc, F., Arendt-Nielsen, L., Ravier, P., Farina, D. Experimental Muscle Pain Changes the Spatial Distribution of Upper Trapezius Muscle Activity During Sustained Contraction. Clin. Neurophysiol. 2006, 117(11), 2436–2445 [viewed 2023-08-03]. Available at: https://doi.org/10.1016/j.clinph.2006.06.753

[64] Abboud, J., Nougarou, F., Pagé, I., Cantin, V., Massicotte, D., & Descarreaux, M. Trunk Motor Variability in Patients with Non-specific Chronic Low Back Pain. Eur. J. Appl. Physiol. 2014, 114(12), 2645-2654 [viewed 2023-08-03]. Available at: 10.1007/s00421-014-2985-8

[65] ACGIH. TLVs and BEIs. 2015. 202-204 ISBN 978-1-607260-77-6.

[66] Luttmann, A., Jäger, M., Laurig, W. Electromyographical Indication of Muscular Fatigue in Occupational Field Studies. International journal of Industrial ergonomics. 2000, 25(6), 645-660 [viewed 2023-08-03]. Available at: https://doi.org/10.1016/S0169-8141(99)00053-0

[67] Rumelhart, D.E.; Hinton, G.E.; Williams, R.J. Learning internal representations by error propagation. In Parallel Distributed Processing; MIT Press: Cambridge, MA, USA, 1986, 1, 318–362.

ISO/IEC 22989:2022-07, *Information technology — Artificial intelligence — Artificial intelligence concepts and terminology*

ISO 29995:2021-05, *Education and learning services — Vocabulary*